



Petit Buëch River Dynamics and Bank Erosion

Analysis by Using Photogrammetry and LIDAR data between 2014-2023

Sercan Yilmaz, s.yilmaz1@students.uu.nl

Supervisor :

Maarten Zeylmans van Emmichoven

Responsible Professor :

Steven de Jong



Contents

Abstract	4
1. Problem and Context	5
2. Research Objectives	7
2.1 Main Research Question	7
2.2 Sub-Research Questions	7
2.3 Research Scope and Limitations	7
3. Methodology	8
3.1 Study Area	8
3.2 Data To Be Used	9
3.3 DSM,DTM and DEM	10
3.4 River Morphology	11
3.4.1. River Types	11
3.4.2. River Channel Morphology	12
3.4.3. Factors Influencing River Morphology	13
3.5 Coordinate Reference System to be used	14
3.6 Processing of Data and Analysis	14
3.6.1. Improving accuracy by co-alignment	16
4. Results	17
4.1 Positional Accuracies, DSMs ,OrthoMosaics.	17
4.2 Volumetric Changes	19
4.3 Channel Displacements	26
4.4 Comparison between data of LIDAR and Photogrammetry	29
5. Discussion	32
6. Conclusions	36
7. References	37

List of Figures

Figure 1: View of part of Petit Buëch River.....	7
Figure 2 : Location and topography of the Petit and Grand Buëch rivers in south eastern France.....	8
Figure 3: Demonstration of captured images	10
Figure 4: Diagram Of Braided River(Dimensions in Biodiversity of a Braided River, 2022).....	11
Figure 5: Example of a meandering river (Meander, n.d.)	12
Figure 6: Generic Workflow Of Structure-From-Motion Approach	14
Figure 7: General steps of generating data through Agisoft Metashape	15
Figure 8: Workflow of Channel Displacement and Accuracy Assessment.....	16
Figure 9: Flow chart of Co-alignment process(Nota et al., 2022).....	17
Figure 10 : UAV derived OrthoMosaic of 2023 in order to indicate the study area	18
Figure 11 : UAV derived DEM of 2023 , indicating inclination trough north to west. Whereas light blue regions shows the high altitude , dark blue areas represent low altitude.	19
Figure 12: Points chosen for representation of river bank and floodplain height for the eroded area between 2015-2014	19
Figure 13 : Calculation average and RMSE of selected points for eroded area between 2015 and 2014	20
Figure 14 : Total eroded area between 2015 and 2014 , which is approximates 6040 m ³	20
Figure 15: A : Points chosen for representation of river bank and floodplain height for the eroded area between 2022-2015 B : Value of the points.....	21
Figure 16 : Eroded areas between 2022 and 2015 . While area in A lost 15550 m ³ , computed erosion is 5777 m ³ in area in B	22
Figure 17 : 2023-2022 small differences based on boundary estimations.	23
Figure 18 : The location of the four transects (A to D) at the bank erosion site between 2023 and 2014. The upper image shows the location of the four transects in the OrthoMosaic of 2022.	24
Figure 19 : Interpretation of profiles	25
Figure 20 : Elevation profiles for the four transects (A to D) in every year.	26
Figure 21 : Channel displacements between 2015 and 2014.....	27
Figure 22: Channel displacements between 2022 and 2015.....	28
Figure 23 : Channel displacements between 2023 and 2022.....	29
Figure 24 : Distribution of points for comparison.....	30
Figure 25 : Comparison point 1 from LIDAR	30
Figure 26 : Comparison point 1 from Photogrammetry	30
Figure 27 : Comparison point 2 from LIDAR	30
Figure 28 : Comparison point 2 from Photogrammetry	30
Figure 29 : Comparison point 3 from LIDAR	31
Figure 30 : Comparison point 3 from Photogrammetry	31
Figure 31 : Comparison point 4 from LIDAR.....	31
Figure 32 : Comparison point 4 from Photogrammetry	31
Figure 33 : Comparison point 5 from LIDAR	31
Figure 34 : Comparison point 5 from Photogrammetry	31
Figure 35 : Comparison point 6 from LIDAR	32
Figure 36 : Comparison point 6 from Photogrammetry	32
Figure 37 : Estimation of river boundary because of hampering by trees.....	33
Figure 38 : Bank lines at the location of bridge in every year , represented on Orthomosaic of 2023.....	34
Figure 39: Eroded volume graph to show disconnected volume values.....	34

List of Tables

<i>Table 1: General information about Petit Buëch river.....</i>	<i>9</i>
<i>Table 2 : Total numbers of photos and markers involved years.....</i>	<i>9</i>
<i>Table 3 : Reference system of project</i>	<i>14</i>
<i>Table 4 : Absolute positional XY accuracy (Euclidean distance in meter) for all years.....</i>	<i>18</i>
<i>Table 5 : Differences between data of LIDAR and Photogrammetry.....</i>	<i>29</i>

Abstract

This study investigates river morphology dynamics and bank erosion along the floodplain of the Buëch River in the Hautes-Alpes province of south-eastern France using multi-temporal images acquired from Unmanned Airborne Vehicles (UAVs) and LIDAR data. Images were captured in June 2014, 2015, 2022, and 2025, and processed using Structure from Motion algorithms to generate high-resolution OrthoMosaics and Digital Elevation Models (DEMs) with a pixel size of 5 cm. The accuracy of these UAV-derived products was assessed using Real Time Kinematic GPS (RTK-GPS) measurements, demonstrating centimeter-level precision in both positional and vertical dimensions. Analysis of the OrthoMosaics and DEMs revealed changes in river channel, including channel displacements and gravel bank movements, with the Buëch River exhibiting primarily braided properties but also sporadic meandering features. Bank erosion volumes were quantified by comparing DEMs from different years as well as calculating the average height difference between floodplain and river bank to estimate eroded volume, particularly in vegetated areas. Mapping of bank retreat was hindered in some instances by factors such as overhanging vegetation, water reflections, and shadows. The findings highlight the utility of time-series high-resolution UAV imagery for river monitoring, offering a flexible and straightforward approach for acquiring valuable data products suitable for land administration and river management. The high accuracy of UAV-derived products in both spatial and vertical dimensions makes them suitable for informing management decisions and designing effective mitigation measures.

1. Problem and Context

Rivers, as one of the most crucial natural water sources on Earth's surface, play a multifaceted role in ecosystems and human societies. They provide transportation routes, sources of energy production, supply water for domestic, agricultural, and industrial use as well as a rich diversity of plant and animal life. However, the delicate balance of these ecosystems can be disrupted by both natural and man-made changes in rivers, leading to various negative consequences. One of the primary challenges facing river ecosystems is the uncontrolled use of water, which can result in reduced water levels and quality (Dimitriou & Stavroulaki, 2018). Additionally, activities like quarrying and the release of pollutants and waste materials into rivers contribute to environmental degradation. These changes in water quality not only affect aquatic life but also human communities that rely on these rivers for drinking water and agriculture. Furthermore, the physical shape of riverbeds is constantly evolving due to the processes of erosion and sediment deposition along the riverbanks. These changes can be influenced by various factors, including seasonal precipitation and temperature fluctuations, leading to shifts in river water levels and causing flooding or drought conditions. The effects of these geomorphological changes can be particularly severe when exacerbated by the impacts of climate change (Kabdaşlı, 2010). Climate change brings about alterations in regional temperature patterns, wind types, precipitation regimes, and air quality. These changes, in turn, lead to variations in temperature, exacerbate extreme weather events, and increase the likelihood of floods and other environmental disasters. Such events have far-reaching consequences, affecting the development and well-being of regions and causing substantial economic and environmental damage. To mitigate the effects of these environmental changes, it is crucial to take proactive measures and carefully monitor and manage river basins. Understanding changes in the banks and the quantity of sediment in rivers can provide valuable insights into predicting and mitigating potential flood events (Tang et al., 2018).

Topographical data is essential in order to assess morphological changes in river basins. While satellite and aerial imagery are effective for monitoring large-scale changes, they may not capture smaller-scale variations that can be equally significant. Unmanned aerial vehicles (UAVs) offer a promising solution in this regard. UAVs are less affected by adverse weather conditions and provide higher flexibility, spatial resolution, and operational cost advantages when compared to satellite imagery. UAV technology has revolutionized the way we can examine morphological changes in river basins. These aircraft can capture high-resolution data, offering a detailed view of riverbeds and the surrounding environment. By utilizing UAVs, it is possible to conduct multi-temporal flights that track changes in riverbanks, erosion rates, sediment deposition, and even flood-related failures (Hemmelder et al., 2018). UAV-based measurements can precisely estimate sediment transport along river channels, a critical parameter for understanding river dynamics and managing potential environmental risks. UAVs have gained popularity in a wide range of applications, presenting a viable alternative to satellite systems for monitoring and modeling Earth's surface. While UAVs have limitations, such as battery life and weather sensitivity, they excel in producing topographic data, especially under challenging weather conditions like cloudy skies. UAVs offer distinct advantages in terms of time efficiency, cost-effectiveness, data acquisition speed, and image

resolution when compared to traditional terrestrial photogrammetry and satellite remote sensing systems. The Structure from Motion (SfM) method, coupled with UAV technology, has significantly improved our ability to analyze and reconstruct complex surfaces in remote areas. Automation in data analysis has made the 3D reconstruction of surfaces more efficient, allowing for rapid change detection analysis (Cucchiaro et al., 2018). UAV-based SfM is proving invaluable in natural hazard monitoring, disaster risk management, emergency response, and security operations. It is particularly useful in assessing areas prone to floods, earthquakes, landslides, geomorphological studies, and volcanic regions, offering high-resolution, cost-effective data for land planning and damage assessment. Through UAVs, high-accuracy digital surface models (DSMs) and OrthoMosaics can be generated with exceptional spatial resolution (Meinen & Robinson, 2020). These technologies are crucial for morphodynamical modeling of rivers, tracking river ecosystems, and estimating the impacts of floods on residential and non-residential regions. Multi-temporal data captured by UAVs allows for the mapping of surfaces where natural or artificial events occur, facilitating the examination of morphological changes and timely response to disasters. In addition to tracking changes in river morphology, UAVs can be used to calculate height differences between DSMs, providing a valuable tool for determining the amount of material transported during landslides or changes in land use and cover in agricultural areas (Pineux et al., 2017). UAV-derived DSM data offers an efficient alternative to traditional measurement methods for monitoring temporal geomorphological changes, particularly in assessing the effects of floods and other environmental events.

It is seen that UAV technology has emerged as a key element in our ability to capture high-resolution data, track morphological changes, and respond swiftly to environmental challenges. By utilizing UAVs and advanced techniques like Structure from Motion, we can better understand, manage, and protect river basins and the ecosystems that depend on them. Furthermore, it is concluded that minimizing morphologic and river basin management issues and creating solutions for river basin conservation is crucial for safe places against bank erosion and flooding, vegetation dynamics, and channel displacement as well as assessing ecological changes (Hemmelder et al., 2018). Thus, a suitable river should be chosen to study to come up with the solution mentioned problems. Since channel displacement and bank erosion are considerable in Petit Buëch River (*Figure 1*), a Natura 2000 area, in the Hautes Alpes province in southwestern France, this selected study area is chosen in order to question the paper's research objectives and questions.



Figure 1: View of part of Petit Buëch River

2. Research Objectives

This research aims to investigate the morphological changes in the Buëch River floodplain between 2014 and 2023 using UAV-based OrthoMosaics, DEM, and LIDAR data. Through analyzing bank erosion rates, channel displacement, and the comparative accuracy of UAV-derived data against LIDAR. Furthermore, this study seeks to enhance our understanding of river dynamics and the potential for predictive modeling in floodplain management by focusing research questions below.

2.1 Main Research Question

How has the Buëch River floodplain's morphology changed in between 2014-2023 derived from UAV based OrthoMosaics, DEM and LIDAR data?

2.2 Sub-Research Questions

1. What are the rates of bank erosion and channel displacement observed over the study period, and how do they vary across different sections of the river?
2. How accurately can UAV-derived data capture river morphology and bank erosion when compared with LIDAR data and its suitability for monitoring river floodplain dynamics?
3. Can predictive models be established to forecast river channel shifts and bank erosion patterns in the Buëch River floodplain?

2.3 Research Scope and Limitations

- The accuracy and precision of the UAV-derived products compared to LIDAR are not extensively assessed for all mentioned years in this study because LIDAR data is just available for 2023.

- The sources of uncertainty in the UAV imagery, such as sun glint and obstructed views, might not be quantified.
- The study focuses on a specific river system and may not be directly applicable to other river ecosystems without further validation.

By analyzing the dynamics of the Buëch River floodplain over the specified period, this research contributes to our knowledge of river's geomorphology . While limitations exist regarding data availability and vegetation cover, this study underscores the importance of integrating advanced remote sensing techniques for comprehensive river ecosystem analysis and predictive modeling.

3. Methodology

3.1 Study Area

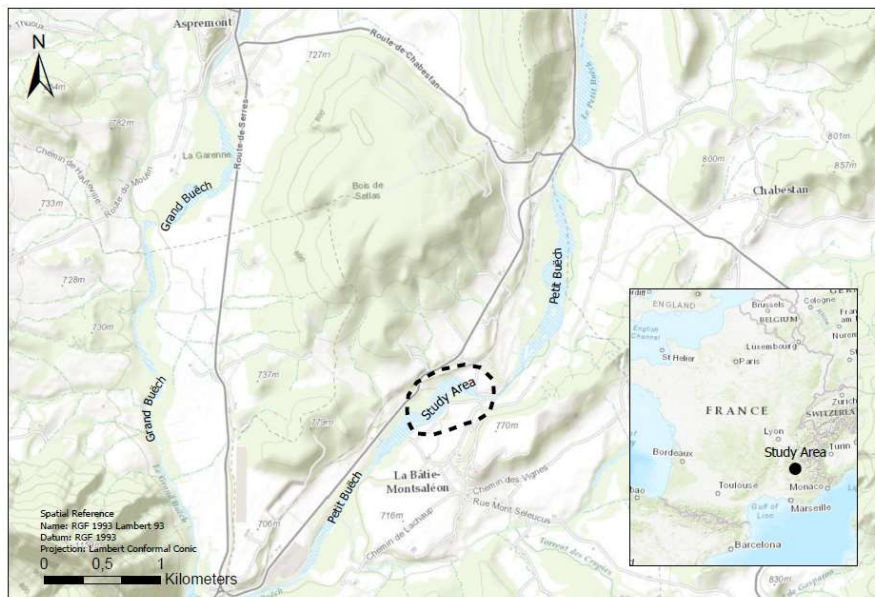


Figure 2 : Location and topography of the Petit and Grand Buëch rivers in south eastern France

The Petit Buëch, as a tributary of the Grande Buëch (Figure 2), plays a crucial role in the overall hydrological system of the region. General information about river indicated in the Table 1 (Vannamettee, 2014). Its discharge pattern, mirroring that of the Grand Buëch, showcases a rhythmic dance of water flow,

with distinct peaks in spring and autumn. The

mean daily discharge of 14.10 m³/s during these peaks as observed (Bertrand et al., 2018), underscores the river's significant contribution to the water network. However, despite its importance, the Petit Buëch experiences a tempered discharge behavior owing to its tributary nature. This characteristic is particularly evident in the summer months when the monthly discharge remains generally low. Conversely, the river sees increased flows in April and October/November, aligning with the seasonal variations documented (Liébault et al., 2013). This nuanced discharge pattern is further influenced by the river's braided stretch, covering approximately 1000m in length and 400m in width. During periods of high discharge, the floodplain of the Petit Buëch becomes a dynamic arena where sediment and suspended loads are intricately shuffled. It is also noted that this process is especially pronounced, emphasizing the river's ability to reshape its surroundings during intense rainfall events and snowmelt in the upper catchment near the Dévoluy massif (Hemmelder et al., 2018). These transformative moments, marked by bank full conditions, offer a glimpse into the river's geomorphic process.

Table 1: General information about Petit Buëch river (Contributeurs aux projets Wikimedia, 2023)

Altitude	680 m
Coordinates	44 ° 26' 55" N , 5 ° 43' 19" E
Localization	Serres
Source	Dévoluy massif
Catchment area	389 km ² (80% Forest and 20% Agricultural Land)
Length	44.5 km

Human activities, such as gravel extraction from quarries near the Buëch, add another layer of complexity to the river's story. Descroix & Gautier (2002) highlight how these quarries directly impact the sediment budget of the Petit Buëch. The extraction of gravel alters the natural flow of sediments within the river, potentially leading to erosion or sedimentation if the delicate balance is

disrupted. This insight into the sediment budget becomes crucial in understanding the long-term environmental implications of human interventions in this ecologically sensitive area. In essence, the Petit Buëch River emerges as a dynamic entity, shaped by the interplay of natural forces and human activities. The delicate balance it maintains, especially in the face of anthropogenic influences, underscores the importance of comprehensive research and sustainable management practices to ensure the resilience and health of this vital ecosystem in the Hautes Alpes province of southwestern France.

3.2 Data To Be Used

The study used a UAV to collect airborne images at La Bâtie field sites, and positional data was collected using the Real Time Kinematic - Global Positioning System (RTK-GPS) Trimble R8 GNSS. The fixed-wing aircraft was manually controlled during the flights, with a Canon PowerShot D10 RGB compact camera for 2014 and 2015 where flight altitude were around 130m. When it comes to 2022 and 2023 flights, they were carried out with DJI Phantom comes with its own built in DJI designed FC6310R camera. Multiple flights were carried out, resulting in hundreds of photographs (*Figure 3*). For La Bâtie, 473 photos were collected in 2014 and 696 in 2015, covering an area of 400 by 1000 m. Additionally, twenty one white markers with an identifiable dark dot were distributed evenly in the study areas. Finally, in 2022 and 2023, 451 and 523 photos were captured respectively (*Table 2*).

Year	Total Number of Photos	Total Number of Markers	Aircraft
2014	473	21	Wing
2015	696	21	Wing
2022	451	21	DJI
2023	523	21	DJI

Table 2 : Total numbers of photos and markers involved years

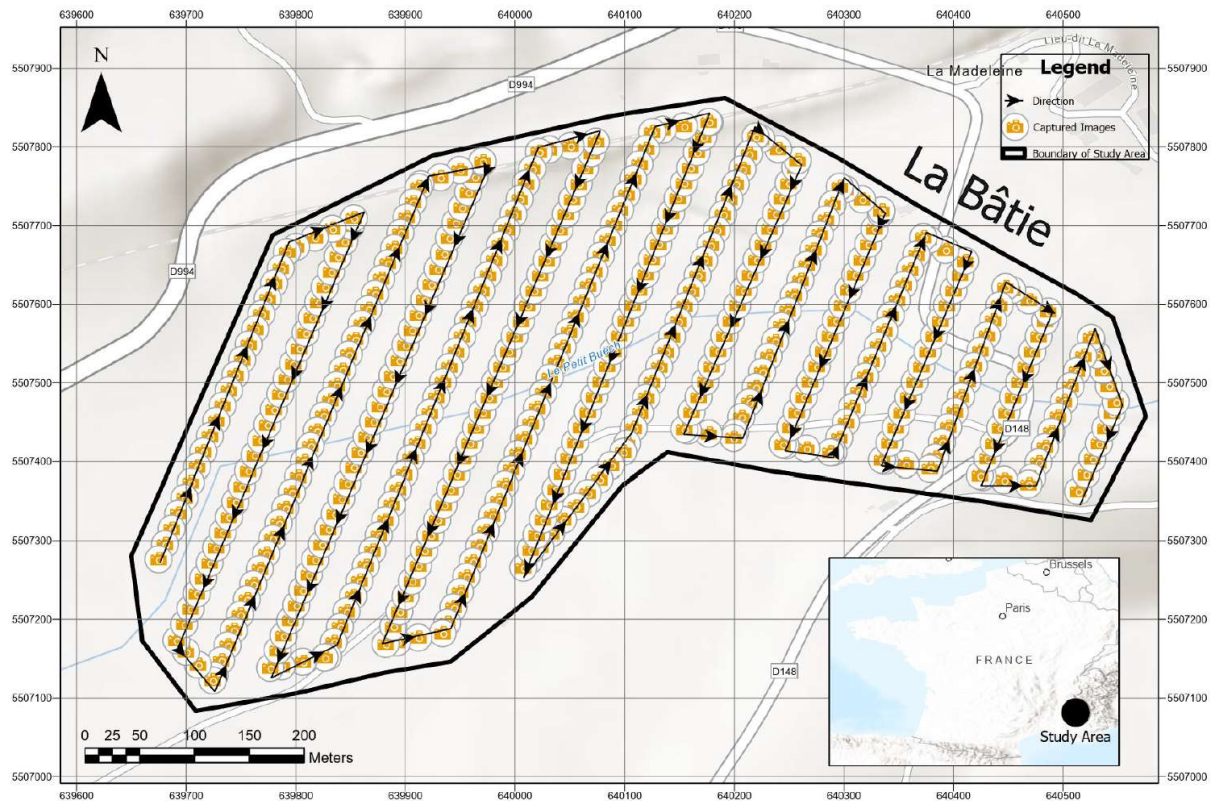


Figure 3: Demonstration of captured images

On the other hand, the LIDAR data can be used as a reference dataset to assess the vertical accuracy of the methods used in the study. By comparing the results obtained from the UAV-derived data with the LIDAR data, the vertical accuracy of the UAV-based measurements can be evaluated. The LIDAR data, which provides high-resolution and accurate topographic information, can serve as a benchmark to validate the accuracy of the UAV-based measurement, which allows the researchers to quantify the errors and uncertainties associated with the UAV-based method and assess its reliability for monitoring and analyzing the morphological changes of the study area (Akay et al., 2019). As a part of the national LiDAR HD program, IGN (*Institut National De L'Information Geographique Et Forestiere*) produces and distributes 3D mapping of the entire ground and subsoil of France in LIDAR data. The data disseminated are in particular clouds of registered points, raw or classified, and 3D digital models. In this research, the latest LIDAR data will be downloaded through IGN website and evaluated to assess accuracy.

3.3 DSM, DTM and DEM

Digital Elevation Models (DEMs) are crucial for analyzing elevation changes (Julzarika, 2019). They provide a representation of the bare Earth's surface without considering features like buildings and vegetation. This makes DEMs particularly useful for applications like hydrological modeling, slope analysis, and landform classification. Now, Digital Surface Models (DSMs) come into play when you need to account for above-ground features such as trees and buildings. Unlike DEMs, DSMs include these surface features in their representation, offering a more comprehensive view of the landscape (Julzarika, 2019). This makes DSMs

valuable in urban planning, forestry management, and telecommunications planning, where understanding the above-ground structures is essential. Digital Terrain Models (DTMs) take things a step further by not only representing the bare Earth's surface but also incorporating additional topographic characteristics like gradient, aspect, and curvatures(Li et al., 2004). These models provide a more detailed and nuanced perspective, making them useful in applications such as geological studies, precision agriculture, and environmental impact assessments.

In essence, DEMs serve as the foundation, providing information about the bare Earth, while DSMs and DTMs build upon this foundation by incorporating above-ground features and additional topographic details, respectively. The choice of which model to use depends on the specific needs of the analysis or application at hand.

3.4 River Morphology

Rivers represent dynamic and intricate systems shaped by a complex interplay of physical processes and environmental factors. In this part of document, river morphology will be addressed in terms of form, structure, and evolution of these watercourses, providing insights into their behavior and the underlying geomorphic processes. In addition, fundamental concepts related to river morphology, focusing on the diverse types of rivers, their channel characteristics, and the dynamic processes governing their evolution will be explored.

3.4.1. River Types

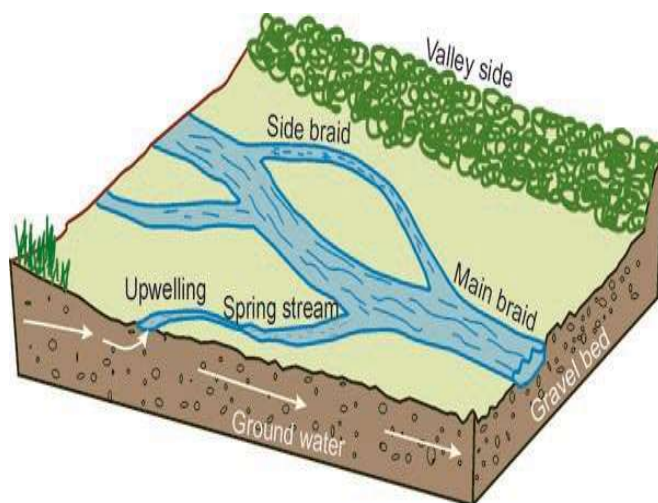


Figure 4: Diagram Of Braided River(Dimensions in Biodiversity of a Braided River, 2022)

Rivers can be classified into various types based on different criteria such as their origin, morphology, geography, and human interaction. In this study , river morphology is analyzed . Thus , river types based on channel morphology will be focused. As rivers are classified in terms of channel morphology , it can be said that there are types of river on modern river plains, some of which are braided , meandering , straight and anastomosing Braided rivers, characterized by multiple intertwining channels, manifest in regions with heightened sediment supply and fluctuating flow conditions and the distinctive braided pattern results in the formation of numerous islands and bars, making these rivers a subject of particular interest in geomorphological studies(Li et al., 2023).

fluctuating flow conditions and the distinctive braided pattern results in the formation of numerous islands and bars, making these rivers a subject of particular interest in geomorphological studies(Li et al., 2023).



Figure 5: Example of a meandering river (Meander, n.d.)

Contrasting with braided counterparts, meandering rivers follow sinuous, single-channel paths across landscapes with moderate sediment supply and gentle gradients (Monegaglia & Tubino, 2019). The development of meanders, or bends, is a characteristic feature, and these rivers play a vital role in shaping floodplains and influencing sediment transport (Monegaglia & Tubino, 2019). Furthermore, while a meandering river typically features a solitary sinuous channel, braided and

anastomosing rivers exhibit multiple intertwining channels (Makaske, 2001). However, unlike braided rivers, where channels are temporary and often shift due to sediment deposition, anastomosing rivers maintain semi-permanent channels separated by floodplain areas instead of channel bars (Makaske, 2001). Lastly, straight rivers exhibit linear channel configurations with minimal bends or curves and they typically occur in regions with uniform geological features and gentle gradients, facilitating straightforward water flow (Sui-ji & Jin-ren, 2002). Straight rivers are prone to erosion and sediment transport, influencing the geomorphology of their surroundings over time (Sui-ji & Jin-ren, 2002). Even though there are other types of river, they are not addressed in this study.

In conclusion, understanding different types of rivers is essential for various reasons, including water resource management, ecological conservation, navigation and transportation, flood prediction and management, recreation and tourism, and recognizing their cultural and historical significance. This enables effective management, conservation, and utilization of river systems, ensuring their sustainability for current and future generations.

3.4.2. River Channel Morphology

Rivers exhibit various channel patterns, including meandering, and braided types. These patterns are intricately linked to factors such as slope, sediment load, and the geological characteristics of the surrounding landscape. Rivers are dynamic entities undergoing continuous evolution. Processes such as incision, terrace formation, and meander migration contribute to the transformation of river channels over time, shaping the landscape and influencing the surrounding environment. Rivers have experienced some process during the year like erosion, transportation, deposition in some circumstances. Rivers erode the landscape through hydraulic action, abrasion, and corrosion (Zarrabi et al., 2021). Understanding these erosional processes is fundamental to unraveling the intricate relationship between rivers and the surrounding terrain. When it comes to transportation, sediment transport downstream is a critical aspect of river dynamics (Hooke, 1979). Furthermore, the deposition of sediments occurs when a river's energy diminishes, leading to the formation of distinctive features such as river bars, floodplains, and deltas. This depositional aspect is a key driver in shaping the physical characteristics of river systems.

3.4.3. Factors Influencing River Morphology

Rivers play key roles in the landscape's evolution because they are a reflection of the complex interactions between several variables. Therefore, in this section, the external forces playing key roles in the forming of shape of rivers and other aspects will be focused on. After exploring the intricacies of these impacting elements, comprehension of the dynamic equilibrium preserved by rivers and the principles guiding their ongoing evolution will be attained. And also, it will be easily seen that as we investigate the variables affecting river morphology man-made and natural forces work together to create the complex fabric of river landscapes. Each component has a serious effect on the morphology of river systems. They range from the general influence of climate on river flow dynamics to the specific effects like geological substrates, tectonic processes, and human interventions. It is important that these influences can be understood in order to figure out the behavior of rivers, sustainable management techniques, and guarantee the preservation of these important natural resources.

There are complex interactions between climate, geology, tectonic activity, and human activity that shape river form(Lewin et al., 2018). Every interaction represents a paramount thread in the evolution of river dynamics(Lewin et al., 2018). Firstly, the climate has a significant impact on precipitation patterns and river flow dynamics, which they shape the morphology of rivers in turn(Ashmore & Church, 2001). As well as the morphology of rivers, changes in sediment transport and erosional patterns result from variations in the climate(Ashmore & Church, 2001). On the other hand, the behavior of a river is greatly influenced by the geological structure of the area, particularly the kind of substrate and bedrock(Sonam et al., 2022). Additionally, a river's morphological features are mostly determined by its ability to withstand erosion and by the presence of silt. Another factor influencing river morphology are tectonic processes which play a significant role in the formation and alteration of landscapes, which affect river channel morphology and topography. Therefore, it can be understood that tectonic influences must be analyzed in order to interpret the long-term evolution of river systems(Vita-Finzi, 2012). When it comes to human activities such as deforestation, urbanization, and the building of structures which are key problems done by humans. The removal of trees along riverbanks, whether for agriculture or urban development, exposes soil to erosion which speed up sedimentation in rivers, altering their shapes over time. Building structures in order to expand urban areas often involves altering river courses for construction purposes which disrupts the natural flow and sediment transport, leading to changes in morphology(McGrane, 2016).

In summary, understanding the dynamic nature of river systems is based on the complex interactions between different river types, channel morphology, and underlying processes. Examining these components offers important insights into how landscapes have changed over time, laying the groundwork for efficient river management, risk reduction, and ecosystem preservation. The foundation for future research into the complex interactions between rivers and the landscapes they pass through is laid out in this chapter.

3.5 Coordinate Reference System to be used

Horizontal	Vertical
Lambert 93 (ESPG: 2154)	RAF90

Table 3 : Reference system of project

French government have a preference to use Lambert 93 coordinate system because of historical, technical, and practical factors. Lambert 93's historical roots trace back to the mid-20th century since French mathematician Lambert devised a conformal conic map projection. This historical background is s a foundation for the system's development and integration into French geospatial practices. First of all , the primary reason behind the French government's preference for Lambert 93 is its accuracy as well as precision tailored to the unique topography of France(Duménieu et al., 2018). As it is known, the conformal projection minimizes distortion by ensuring high accuracy crucial for mapping diverse landscapes(Pędzich, 2005). This precision is essential for various applications including cartography, urban planning, and development of infrastructure. Furthermore, the adoption of Lambert 93 ensures seamless integration across sectors. From cartography to urban planning and infrastructure development, the standardized coordinate system simplifies processes and promotes consistency in geospatial practices. The technical aspects of Lambert 93 contribute to its sustainability as a geodetic datum with the help of conformal projection and grid system . The system's association with geodetic datums ensures adaptability to changes in Earth's shape over time , which address long-term considerations in geospatial data management.

In essence, it can be understood that the French government's choice to use Lambert 93 is a strategic decision based on historical development, technical efficacy, and the practical needs of various sectors. This coordinate system aligns with the unique geographical features of France and positions the country for effective collaboration within Europe and the global geospatial community.

3.6 Processing of Data and Analysis

The main method of this research is photogrammetry aiming at a virtual landscape reconstruction of the floodplain. By matching the objects in the photo series with varying overlap rates, taken at different places, the Structured from Motion(SfM) method, a new, quick, and inexpensive photogrammetric method, delivers high accuracy three-dimensional data(Colomina & Molina, 2014). Bundle adjustment is used to determine parameters with high accuracy and improve SFM method since it offers camera locations and extracts 3D positions of objects. The general workflow of Structure From Motion is described like *Figure 6*.

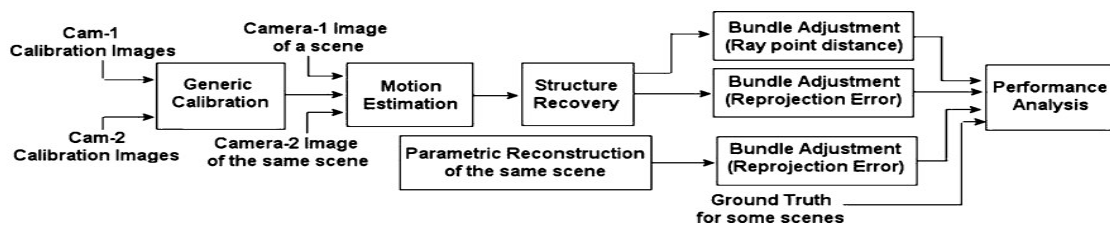


Figure 6: Generic Workflow Of Structure-From-Motion Approach (Ramalingam et al., 2006)

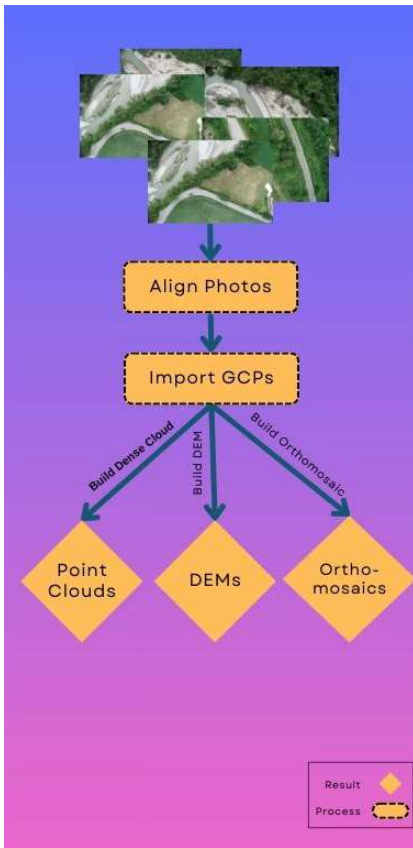


Figure 7: General steps of generating data through Agisoft Metashape

Bundle adjustment also makes sure that the cost function is kept to a minimum (Zhang et al., 2006). In order to analyze two-dimensional (2D) and three-dimensional (3D) morphological changes of the surfaces, the SfM approach produced point clouds, DSMs, and OrthoMosaics, which can provide highly valuable data in many different large- and small-scale investigations (Akay et al., 2019). The acquired UAV photos will be processed into a Digital Elevation Model (DEM), Point Clouds and OrthoMosaic (Figure 7) using Agisoft Metashape Professional utilizing SfM (Agisoft, 2023). These models for every mentioned year will be georeferenced based on all markers identified in the images. Only taking into consideration sharp, non-blurred, overhead angles aerial images captured by UAVs will be used. Marked specific points in these images and their positions were accurately measured using RTK-GPS. To create a coherent 3D model, alignment process is carried out. This alignment process produced a sparse point cloud after removing any obviously incorrect points from it. Subsequently, scaling up this sparse point cloud to generate a high-quality dense point cloud consisting of millions of points is another step. From this dense point cloud, a detailed surface mesh is created. This mesh is then further refined to produce a georeferenced Digital Elevation

Model (DEM) and OrthoMosaic by projecting the original images onto the 3D surface. In order to improve results co-alignment technique will be key element, which is elaborated in next section (3.6.1).

The OrthoMosaics and DEMs will be used to qualitatively assess channel displacements and bank erosion. After digitizing OrthoMosaics, by measuring the distance between the outside borders of the main channels and comparing it with the outer borders of channels in years for each stretch where the channel was moved, the channel displacements will be identified (Figure 8-A). The next step is to quantify channel displacement by comparing the largest difference in channel location between these years. On the basis of river-perpendicular transects at bank erosion sites produced from the DEMs, bank erosion will be quantified and compared. The amount of material that has been degraded will also be estimated (Hemmelder et al., 2018). In addition, the volume of eroded earth material can be calculated by subtracting the two DEMs for this polygon area (Hemmelder et al., 2018). However, the results obtained by SfM method produces DSMs including vegetation cover which hamper to analysis volumetric changes. Thus, the surface area of the eroded bank was multiplied by the average bank height defined outside the forested region to calculate the eroded volume.

On the other hand, LIDAR data will be a part of analysis with help of comparison of point clouds derived by both methods. This comparison will be done by analyzing the differences in the elevation values and the spatial distribution of the features acquired by both methods by overlaying each other (Figure 8-B). Therefore, 6 points will be distributed to assess differences between these datasets.

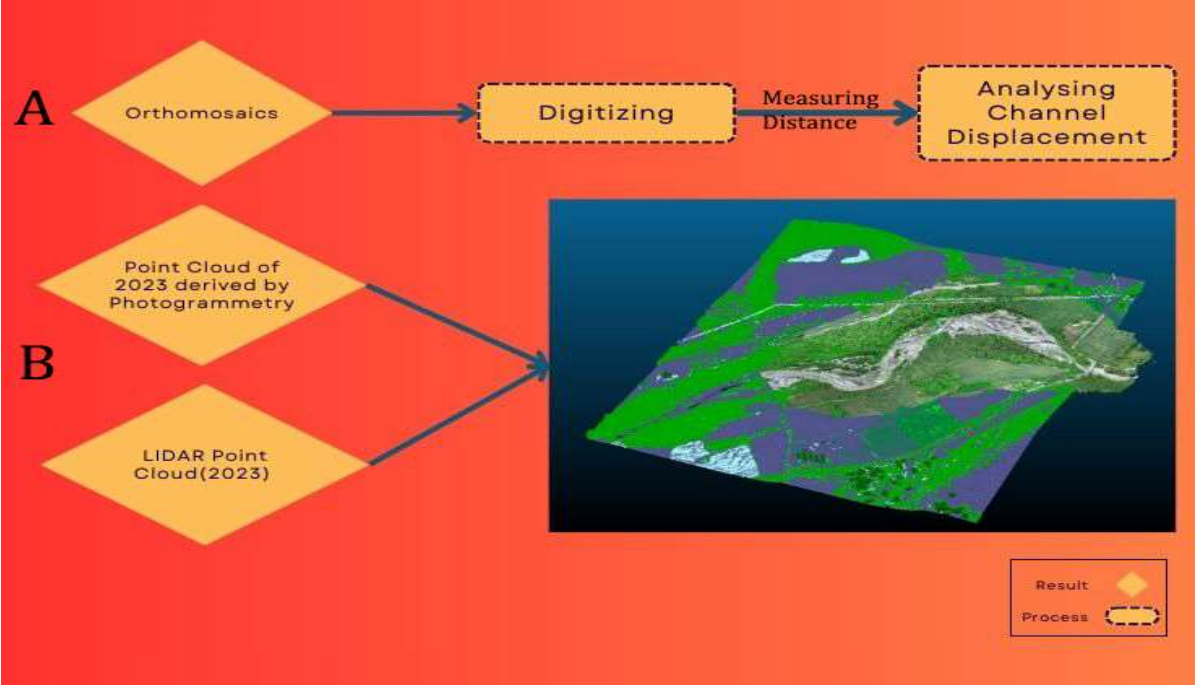


Figure 8: Workflow of Channel Displacement and Accuracy Assessment

When it comes to predictive models for forecasting river channel shifts and bank erosion patterns, it can be developed using historical data, but the effectiveness of such models depends on various factors, including the complexity of the river system, the quality and quantity of available data, and the modeling techniques used. In addition, river systems are highly dynamic, and their behavior can be influenced by numerous factors, including climate, land use, and human activities. The complexity of the predictive model should be tailored to the complexity of the river system. Simple statistical models (e.g., linear regression) may be suitable for relatively stable rivers, while more complex models (e.g., hydrodynamic models) may be needed for highly dynamic systems. Thus, models will be evaluated to figure out which they are suitable for La Bâtie river.

3.6.1. Improving accuracy by co-alignment

The primary aim of co-alignment is to enhance the accuracy of Digital Surface Models (DSMs) generated through Unmanned Aerial Vehicle Structure-from-Motion (UAV-SfM) photogrammetry. And, co-alignment is also a robust method for comparing point clouds in change detection (Saponaro et al., 2021). Co-alignment is utilized to create multi-temporal models by processing UAV imagery from multiple surveys as a single block during the alignment step (Feurer & Vinatier, 2018). After alignment all of the images together, they are separated to blocks again for further steps (Figure 9). This method aims to improve the relative

positioning of DSMs, reduce errors, and enable change detection on smaller scales than previously possible. Additionally, co-alignment aims to provide a robust method for comparing point clouds in change detection studies and to improve the accuracy of DSMs, particularly in scenarios with mixed positioning precision and different sensor grades (Nota et al., 2022). Moreover, co-alignment is beneficial for improving the accuracy of DSMs of older surveys conducted with lower-quality sensors and UAVs, by co-aligning them with one RTK survey where GCPs are digitized towards an RTK accuracy. These circumstances are consistent with our research, since different sensors were used in these four years. And also, there is one RTK survey carried out in 2023.

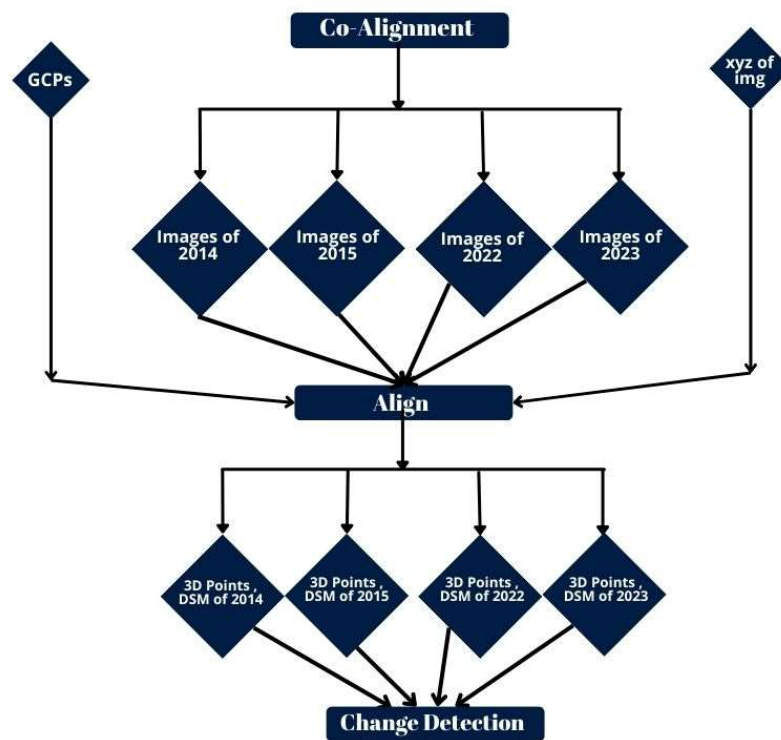


Figure 9: Flow chart of Co-alignment process (Nota et al., 2022)

4. Results

4.1 Positional Accuracies, DSMs, OrthoMosaics.

Within the project's duration in 2014, 2015, 2022, and 2023, a total of 473,696,451,523 photos were collected. However, a meticulous selection process was employed, and only 462,619,446,456 photos met the criteria for inclusion. Therefore, 1983 photos were used in total for improved result through co-alignment technique. The primary focus was on sharpness and clarity to ensure the highest quality data for accurate photogrammetric processing. Ground control points played a pivotal role in maintaining precision throughout the project. Out of the 21 identified points, 13 were actively utilized in the photogrammetric

process. Including these points was crucial for aligning the imagery and enhancing the overall accuracy of the final model. The photogrammetric process itself involved intricate steps, transforming raw data into valuable insights. Following the construction of the point cloud, Digital Elevation Models(Figure 11) and OrthoMosaics(Figure 10) were generated for all years. A pixel size of 5 cm was applied consistently across these outputs. The emphasis on maintaining this uniform pixel size ensures precision and consistency in the representation of the terrain or objects in the generated models and OrthoMosaics. Generating OrthoMosaics provides possibility to evaluate the positional accuracy in XY and Z direction(Table 4.) It is carried out to measure the Euclidean distance between the GCP's coordinates measured and estimated positions of them in the modelled OrthoMosaics.

Year	XY(cm)	Z(cm)
2014	± 7	± 3
2015	± 9	± 3
2022	± 8	± 11
2023	± 8	± 12

Table 4 : Absolute positional XY accuracy (Euclidean distance in meter) for all years

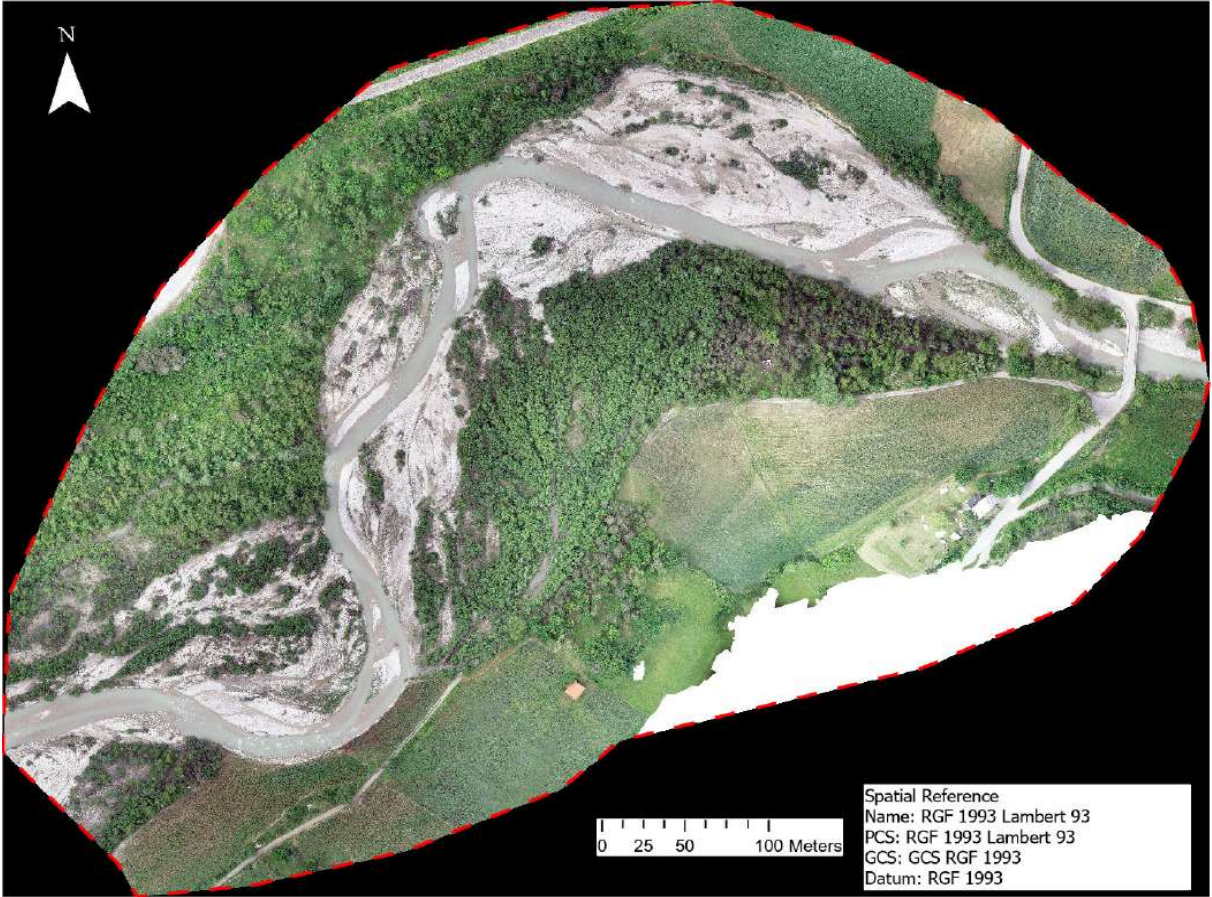


Figure 10 : UAV derived OrthoMosaic of 2023 in order to indicate the study area

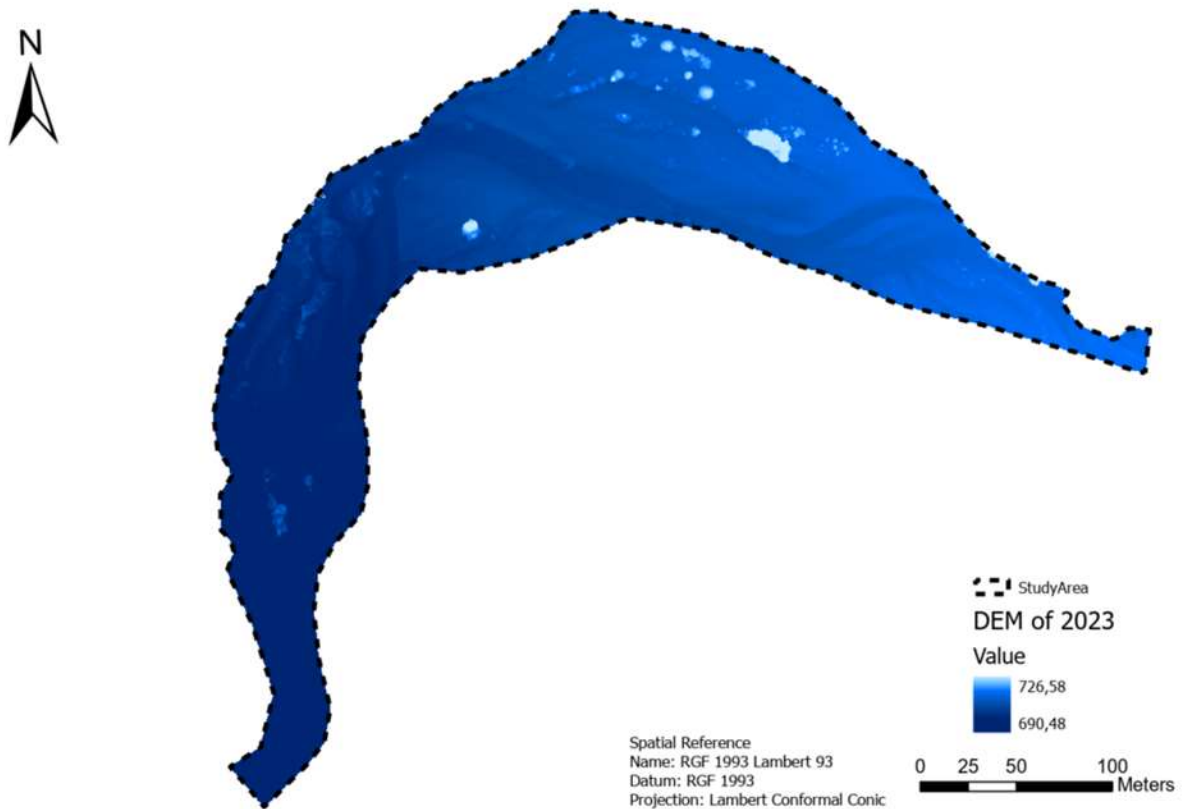


Figure 11 : UAV derived DEM of 2023 , indicating inclination trough north to west. Whereas light blue regions shows the high altitude , dark blue areas represent low altitude.

4.2 Volumetric Changes

The erosion volume and bank retreat was quantitatively determined with some steps. Defining the eroded area by overlapping boundaries of river channel digitized from OrthoMosaics was the first step. The total surface area of the retreated bank multiply by river bank height minus the floodplain height. However , these heights were not measured directly because of



Figure 12: Points chosen for representation of river bank and floodplain height for the eroded area between 2015-2014

vegetation cover, toppled trees and shrubs in the river. Thus, 5 points outside of the vegetated area for river bank height and 5 points for floodplain height were taken into account and averaged in order to decrease inaccuracies. Furthermore, choosing appropriate points process should be carried out carefully in order to represent intended surface .River banks height points were chosen by taking being close to the

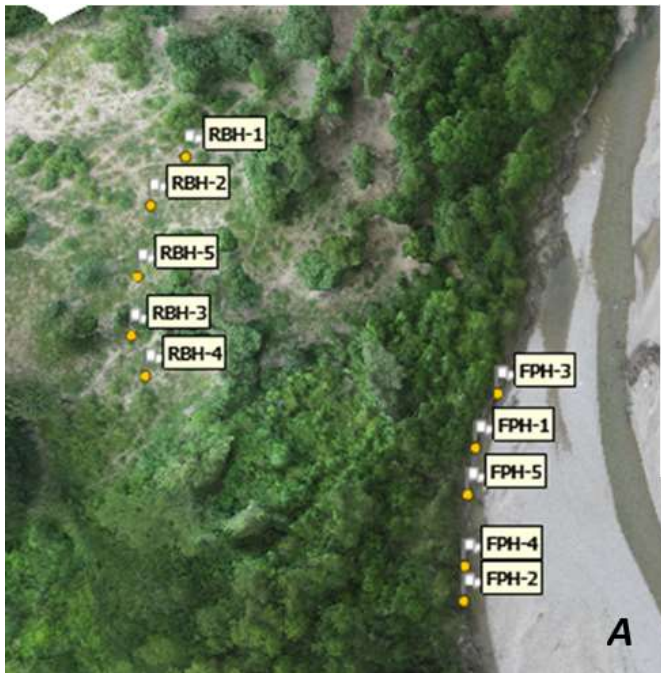
FloodPlain	(m)	Average	RMSE
FPH-1	699,98	699,93	0,08
FPH-2	699,86		
FPH-3	699,99		
FPH-4	699,81		
FPH-5	700,02		
River Bank		Average	RMSE
RBH-1	701,77	701,88	0,12
RBH-2	701,92		
RBH-3	701,73		
RBH-4	702,03		
RBH-5	701,97		

Figure 13 : Calculation average and RMSE of selected points for eroded area between 2015 and 2014

eroded area into consideration. Floodplain height points were selected out of area including toppled trees and shrubs. Figure 12 indicates the points defined by with these rules. The former is 701,88 m. \pm 0,12 m. and the latter is 699,93 m. \pm 0,08 m. for differences between 2015 and 2014(Figure 13). After these ,eroded volume between 2015 and 2014 was assessed obeying this rules. Figure 14 indicates a blue dashed area west of the river that was eroded in the 2015 image. The dimensions of the eroded area are approximately 170m up to a maximum of 45m perpendicular on the channel. The total eroded volume is approximates 6040 m³ \pm 492 m³ and its surface area is 3473 m².



Figure 14 : Total eroded area between 2015 and 2014 , which is approximates 6040 m³ .



FloodPlain	(m)	Average	RMSE
FPH-1	699,98	699,93	0,08
FPH-2	699,86		
FPH-3	699,99		
FPH-4	699,81		
FPH-5	700,02		
River Bank		Average	RMSE
RBH-1	701,94	702,06	0,14
RBH-2	701,86		
RBH-3	702,23		
RBH-4	702,11		
RBH-5	702,16		

Figure 15: A : Points chosen for representation of river bank and floodplain height for the eroded area between 2022-2015
 B : Value of the points

Even though there are really small changes between 2023-2022, eroded part of the river extended at the upcoming years. Red dashed area indicates the eroded part between 2022 and 2015. With the same average technique , heights for calculations

were acquired(Figure 15-A). The river bank height is $702,06 \pm 0,14$ m. and floodplain height is $699,93 \pm 0,08$ m.(Figure 15-B) The dimensions of the eroded area are approximately 235m up to a maximum of 40m perpendicular on the channel ,which covers 7302.92 m^2 . $15550 \text{ m}^3 \pm 1174 \text{ m}^3$ river bank eroded between 2022-2015 (Figure 16A).There is also another eroded area of the river's west part(Figure 16B). The eroded volume of this area can be calculated easily by subtracting DEM of 2022-2015 since there is no vegetation cover. Computed volume is 5777 m^3 (Figure 16B).

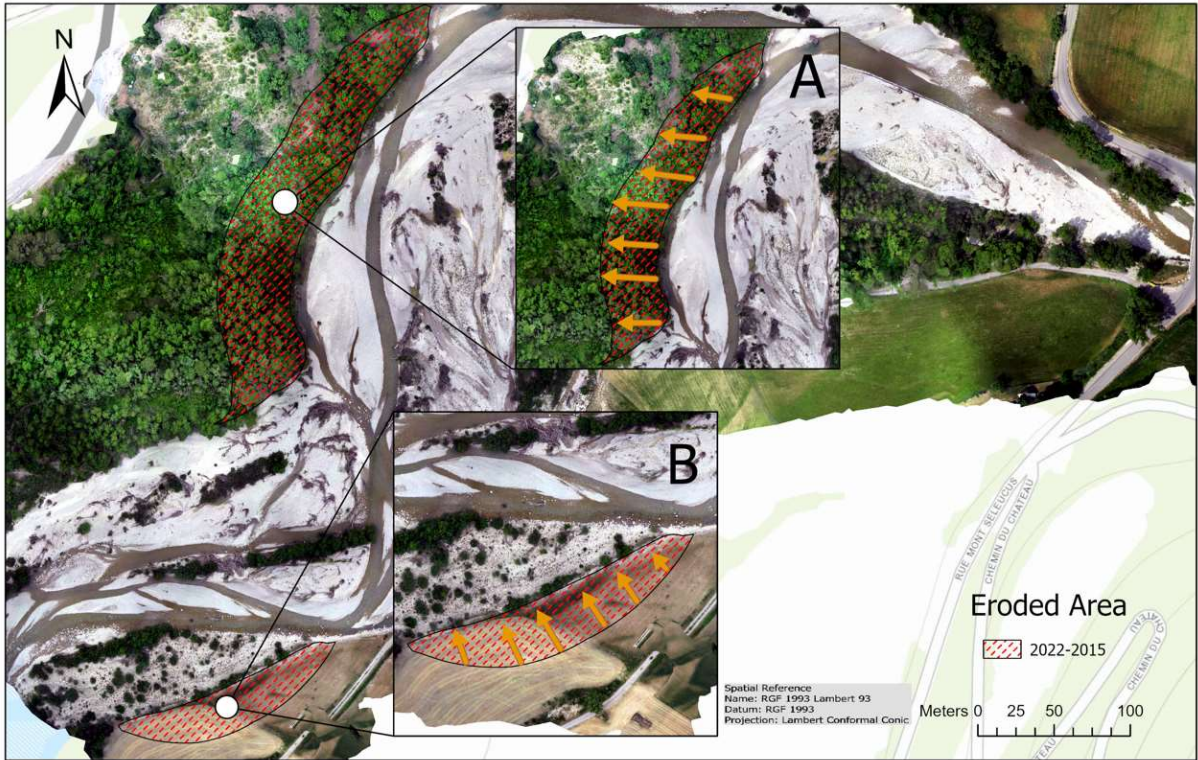


Figure 16 : Eroded areas between 2022 and 2015 . While area in A lost 15550 m^3 , computed erosion is 5777 m^3 in area in B .

There has not been considerable changes between 2023-2022. However , it seems some discrepancies on river boundaries(*Figure 17*). The reason is based on digitizing problem since only average boundaries can be acquired because of growing , toppled trees and shrubs.

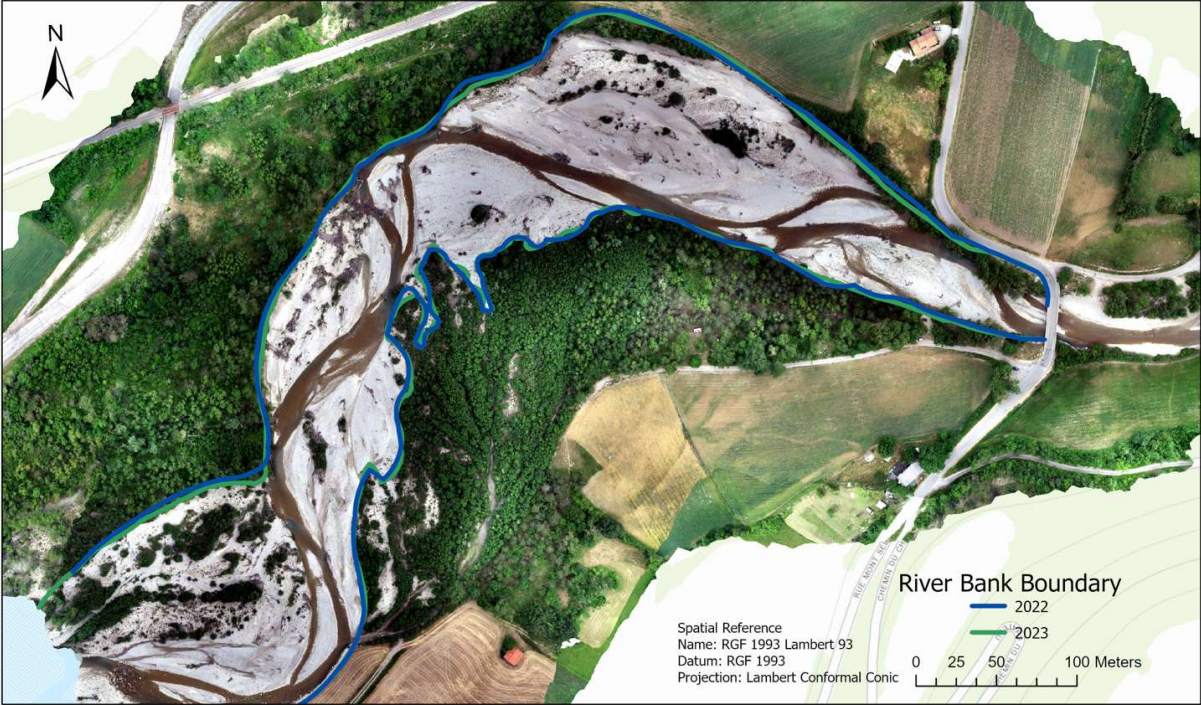


Figure 17 : 2023-2022 small differences based on boundary estimations.

In addition to volume estimation of eroded river bank material with the help of multitemporal OrthoMosaics , DEMs are useful for evaluating profiles of bank erosion. A site of active bank erosion was selected at west part of the river to illustrate the procedure (*Figure 18A*). This site is characterized by a steep edges and have ongoing erosion throughout study duration. Four transects were selected in the images perpendicular on the river channel. Fig.18B-E shows the locations of these transects on the OrthoMosaics of four years respectively. When transects are inspected , although there is river bank in 2014 and 2015 , there are two channels two channels in 2022 and 2023.

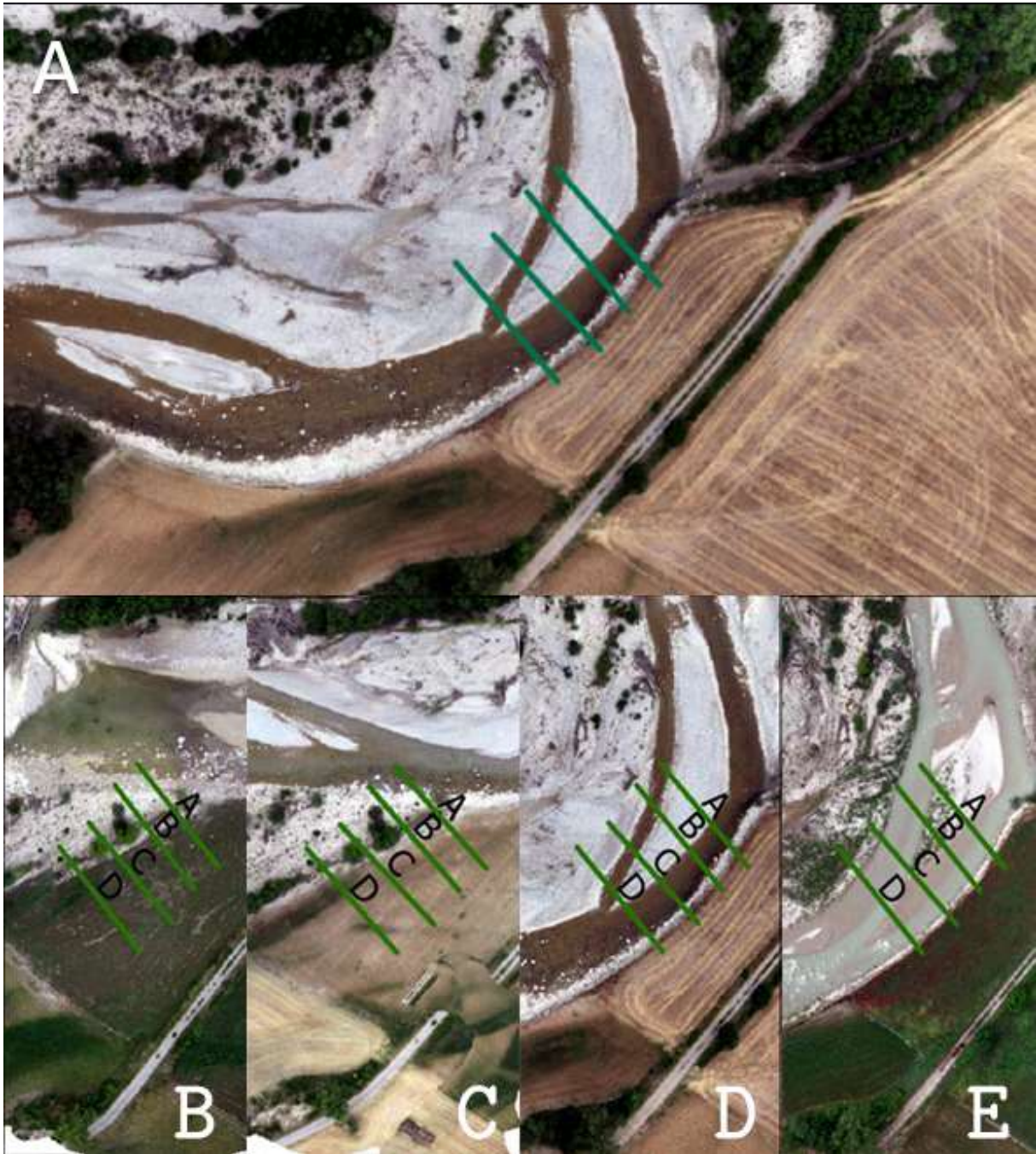


Figure 18 : The location of the four transects (A to D) at the bank erosion site between 2023 and 2014. The upper image shows the location of the four transects in the OrthoMosaic of 2022.

Figure 20 shows the elevation profiles for these four transects derived from the DEMs, color of every line represents different years. Fig. 18B-E shows deepening of the channels and retreating river bank. Channel depth is not certainly defined because of the glitter and mirroring effects of the water. However ,active ongoing sedimentation and erosion processes can be easily seen in the profiles and OrthoMosaics. Thus, the retreating banks are clearly visible in the four transects.

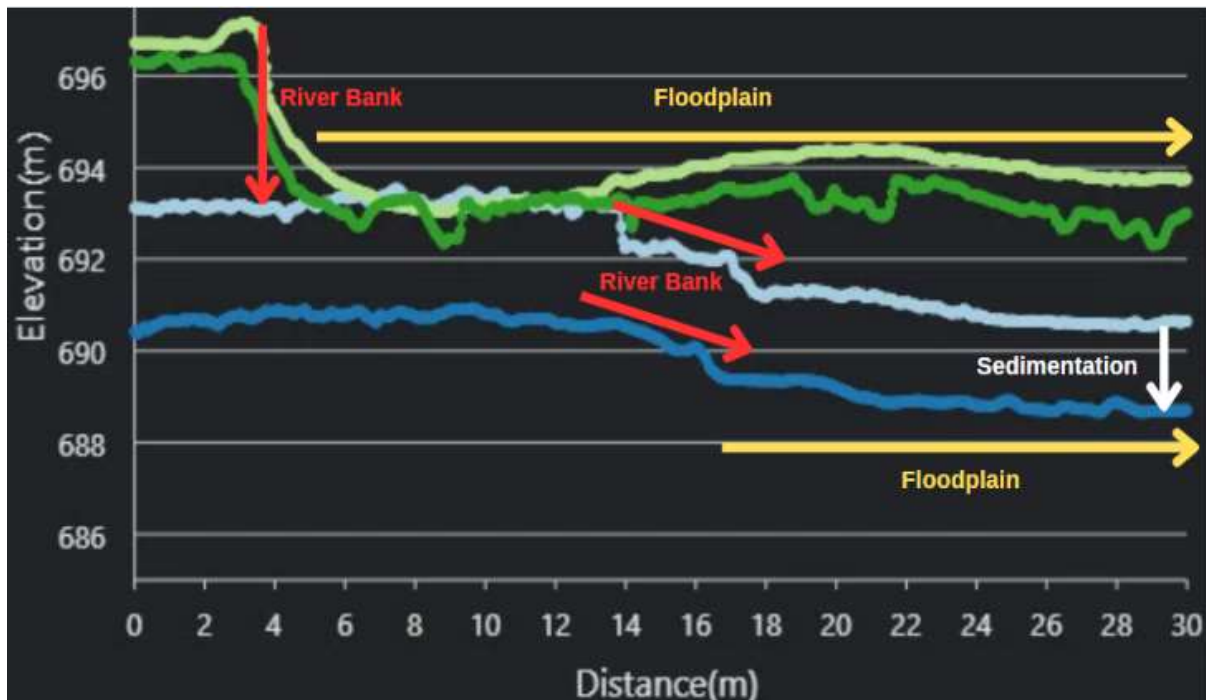


Figure 19 : Interpretation of profiles

Firstly , it should be known how interpret the profiles. Sharp elevation differences indicates river bank as the profile lines encounter considerable elevation decrease when passing through river bank(Figure 19) .After identifying river bank location , amount of retreatment can be calculated by subtracting river bank location between years. Furthermore , floodplain is represented relatively flat line after river bank. Sedimentation is also estimated comparing elevation differences between floodplain(Figure 19). Furthermore ,at the upper left of profile (Figure 20A) around 2 meters of sediment was deposited between 2015 and 2014 . However, there are relatively small deposited sediment monitored between 2023 and 2022. It is also evident that there is 12 meters retreating on the river bank as sharp elevation differences compared . Although, there is significant decrease at the 2 meters distance of profile in the 2023 and 2022 , relatively smooth decrease is observed at the 2015 and 2014 at 14 meters distance of profile. In addition , river bank height declined around 2 meters between 2015 and 2014 while there is around 15 cm decrease between 2023 and 2022. This patterns is same for profile B(Figure 20B). When it comes to the lower left(C) and right of profile(D) (Figure 20C-D), there is around 20 meters shift in the river banks. Whereas, river bank height fell of around 2,5 meters between 2015 and 2014 , there is also 1 meter drop between 2023 and 2022. Sedimentation is also observed in these profiles around 1.5 meter in both profiles and compared years. Additionally, there is a sharp rise in profile C at the 24 meters of distance since one of the small tree lead increase in the DEM(Figure 20C).Nevertheless ,these analyses cannot be carried out along the entire river as vegetation cover on the river bank and tumbled trees in the channel hamper an open view and complicate the identification of bank erosion , which problems also addressed by Tamminga et al., (2015). Complete identification of bank erosion is only possible in open, vegetation free sites.

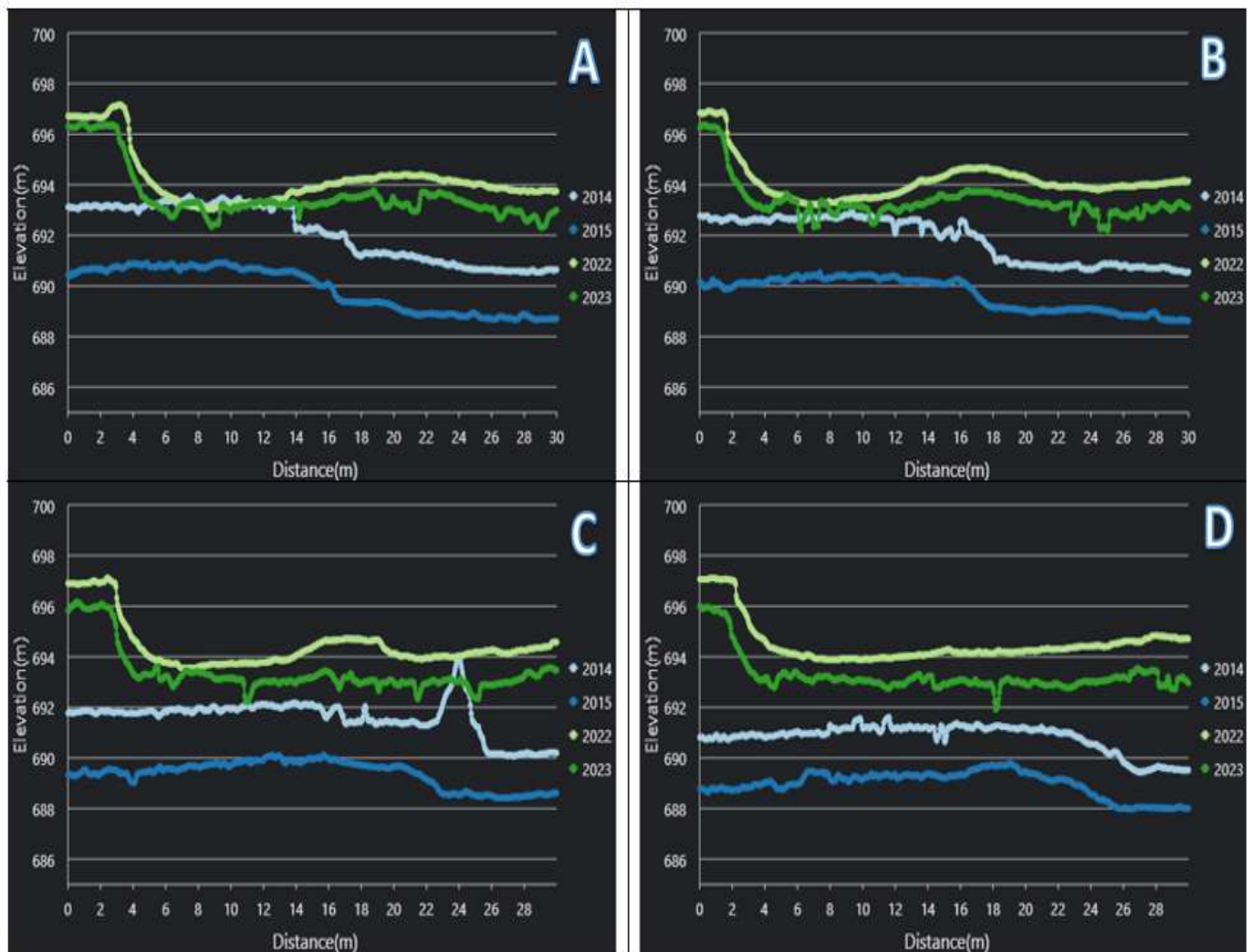


Figure 20 : Elevation profiles for the four transects (A to D) in every year.

4.3 Channel Displacements

The Buëch river exhibits a low discharge during image acquisition, facilitating clear observation of its morphological features. Originating from the east and flowing westward, the river's management upstream of the bridge directs its flow into a single channel, where braiding and meandering processes manifest beyond the bridge. Braided rivers, characterized by their intricate geometry, feature two or more adjacent channels that repeatedly split and merge, forming distinct bars or islands. This braiding phenomenon is intricately linked to the river's transport capacity: when the river lacks sufficient energy to carry its entire sediment load, coarser particles settle, forming bars and dividing the flow. Visible in the Buëch are various active, abandoned, and ephemeral channels, alongside elongated ridges of gravel banks, vividly illustrating the river's braided behavior. In contrast, meandering rivers exhibit smooth bends of similar size, typically found in channels with fine-grained sediments and low gradients. Meanders represent the river's response to resistance and the uniform dissipation of energy along its path. Although the local gradient of the Buëch river is relatively small, measuring less than 3%, its sediment composition is neither uniform nor fine-grained. Consequently, the river tends towards a more braided rather than meandering behavior, as noted by Allen (2012).

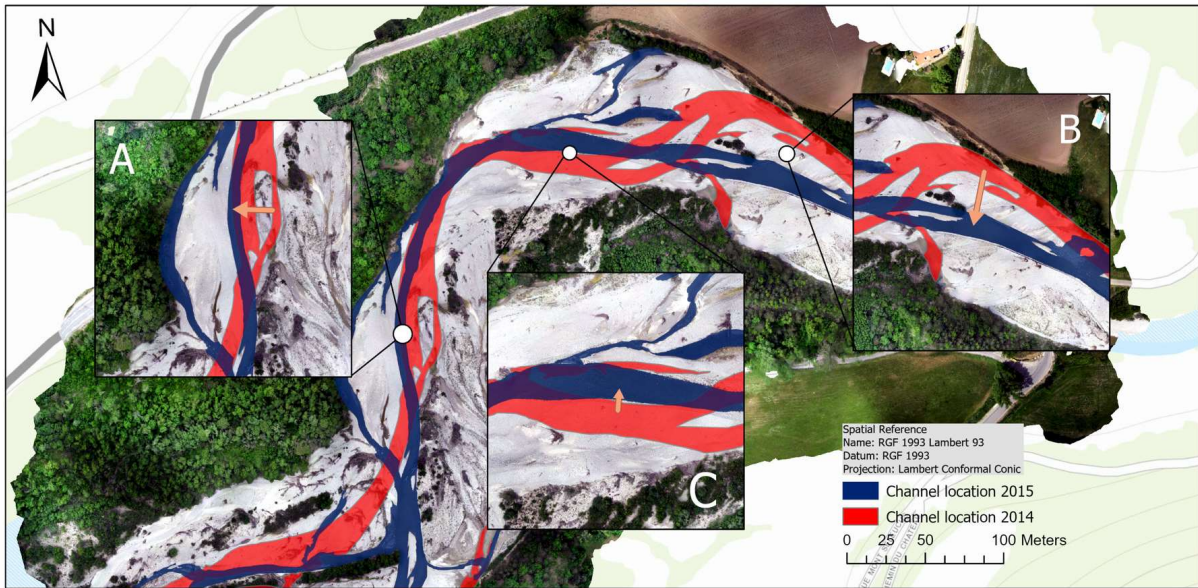


Figure 21 : Channel displacements between 2015 and 2014 . Channels of 2014 and 2015 are represented red and blue ,respectively .

Channel displacements between 2015 – 2014 are presented on the OrthoMosaic of 2015 (Figure 21). Over the course of one year, notable channel displacements of 22, 30, and 15 meters have been observed for the three respective boxes denoted as Figure 21A, B, and C. The geographical dynamics surrounding box A are particularly significant, as a substantial portion of the river bank, adorned with dense forest cover, succumbed to erosion within this brief timeframe. The repercussions of this erosion are evident downstream, where the floodplain now bears the traces of many tree trunks displaced from the eroded site. The Buëch River, currently in a state of erosion and migration towards the north in its central region, poses a substantial threat to the infrastructure of the Veynes to Serres railroad, situated a mere 30 meters north of the actively shifting channel. This northward migration of the river, if unabated, holds serious implications for the stability and safety of the railroad. The erosion-induced displacement of the river channel necessitates careful monitoring and potential mitigation strategies to safeguard the integrity of the crucial transportation route. Contrastingly, in box C, channel displacement unfolds within the existing floodplain without causing significant damage or erosion to the banks. The relatively stable conditions in this area present a notable departure from the challenges faced by box A, emphasizing the localized nature of channel dynamics along the Buëch River. Understanding these variations is crucial for implementing targeted measures to mitigate the risks posed to both natural habitats and critical infrastructure.

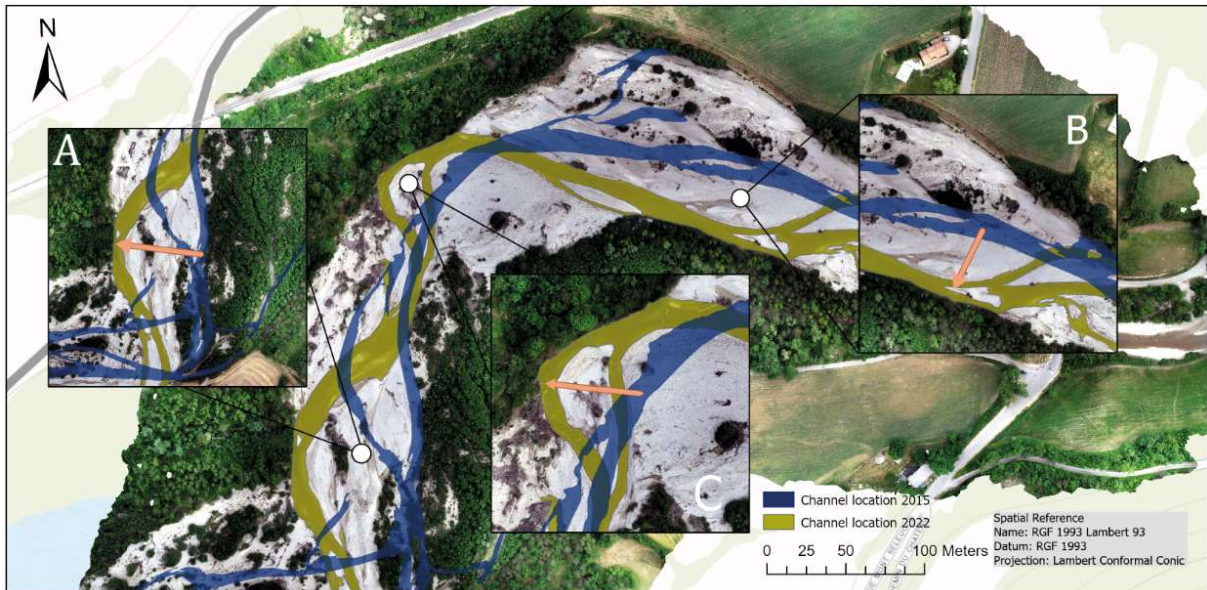


Figure 22: Channel displacements between 2022 and 2015

Channel displacements continued between 2022 and 2015 as well (Figure 22). Over the course of a single year, substantial channel displacements have been observed for three distinct locations along the Buëch river. Box A experienced a noteworthy displacement of 70 meters, while Box C and Box B encountered displacements of 45 and 36 meters, respectively. These displacements have had diverse impacts on the surrounding environment, with significant consequences for the river banks and floodplain. At the sites of Boxes A and C, the river's erosive forces have led to the substantial loss of forested riverbank areas. The erosion has been so severe that a considerable portion of the riverbank, covered with lush vegetation, has been worn away over the course of the year. The consequence of this erosion has been the deposition of numerous tree trunks downstream in the floodplain, a visible testament to the forceful transformation occurring along the Buëch. In stark contrast, the displacement observed in Box B has unfolded within the existing floodplain, demonstrating a more controlled and less damaging process. In this location, the channel has shifted without causing erosion or damage to the river banks. The natural evolution of the river's course within the floodplain has allowed for a more stable and sustainable adaptation without the pronounced environmental impact witnessed in Boxes A and C. It is crucial to note that the central part of the Buëch is currently undergoing a northward migration, contributing to the dynamic changes observed in the river's course. These channel displacements underscore the complex interplay between natural geomorphic processes and the vulnerability of riverbank ecosystems. The juxtaposition of erosive forces and the more subdued displacement in Box B highlight the nuanced dynamics at play within the river system.

Additionally, between 2022 and 2023, the Buëch River underwent subtle channel displacements, characterized by the separation of its channels. Unlike the significant shifts observed in the previous year, these changes manifested as a nuanced interplay of narrowing (Figure 23B) and enlargement (Figure 23A-C) along various sections of the river. This dynamic behavior adds complexity to the river's evolving landscape. The consequences are observable in the physical separation of the channels, reflecting ongoing geomorphic processes influencing water flow and sediment transport. Comparing these nuanced

displacements with the dramatic events of the previous year highlights the multifaceted nature of the Buëch River's behavior. This understanding emphasizes the need for continuous monitoring and research for informed environmental management, considering the varied impacts on the river ecosystem and adjacent landscapes over time.

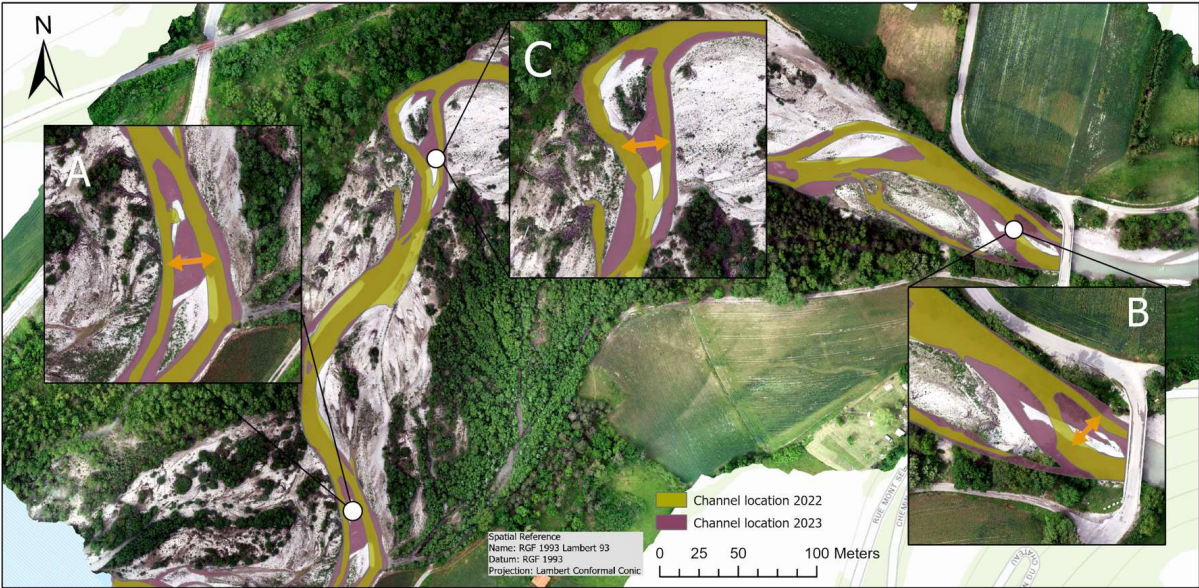


Figure 23 : Channel displacements between 2023 and 2022

4.4 Comparison between data of LIDAR and Photogrammetry

6 points were distributed to area to asses differences between datasets, which differences represent the deviation between the LIDAR and Photogrammetry elevation values for each point (Table 5). Distribution of these points were carried out by ensuring cover of study area. When it comes to interpreting , positive differences indicate that the LIDAR value is higher, while negative differences indicate that the Photogrammetry value is higher. These differences can be analyzed to understand the level of agreement or discrepancy between the two datasets. If the differences are small, it suggests good agreement between the methods. If there are larger differences, it may be worth investigating the reasons behind them, such as the accuracy and precision of each method or potential errors in data processing.

Point ID	Elevation		Difference (cm)
	LIDAR	Photogrammetry	
Cmprsn-1	708.20 m.	708,15 m.	5
Cmprsn-2	711.65 m.	711.72 m.	-7
Cmprsn-3	711.66 m.	711.71 m.	-5
Cmprsn-4	702.20 m.	702.13 m.	7
Cmprsn-5	710.05 m.	710.02 m.	3
Cmprsn-6	705.41 m.	705.32 m.	9

Table 5 : Differences between data of LIDAR and Photogrammetry

LIDAR	Photogrammetry
-------	----------------

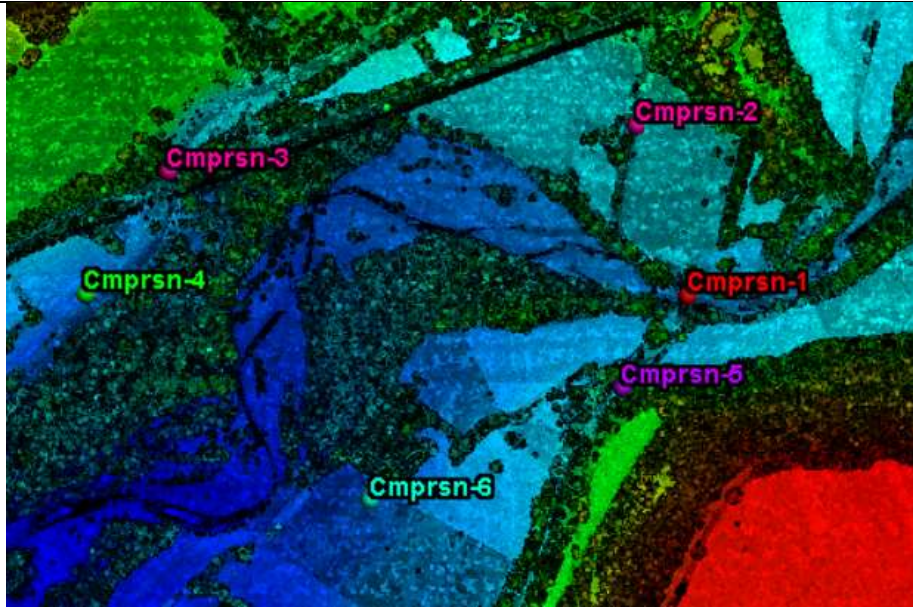


Figure 24 : Distribution of points for comparison



Figure 25 : Comparison point 1 from LIDAR



Figure 26 : Comparison point 1 from Photogrammetry

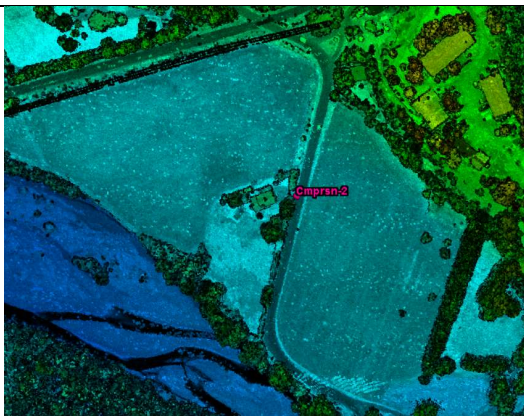


Figure 27 : Comparison point 2 from LIDAR



Figure 28 : Comparison point 2 from Photogrammetry

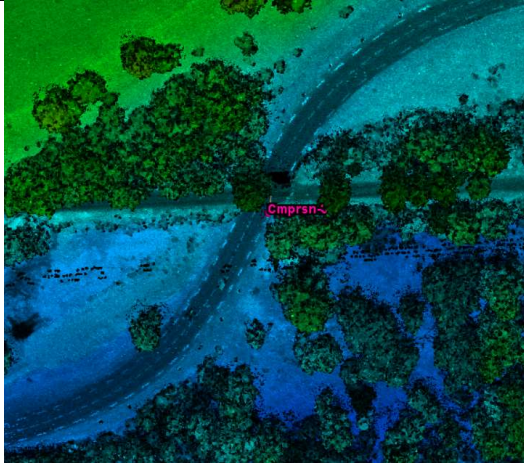


Figure 29 : Comparison point 3 from LIDAR



Figure 30 : Comparison point 3 from Photogrammetry



Figure 31 : Comparison point 4 from LIDAR



Figure 32 : Comparison point 4 from Photogrammetry

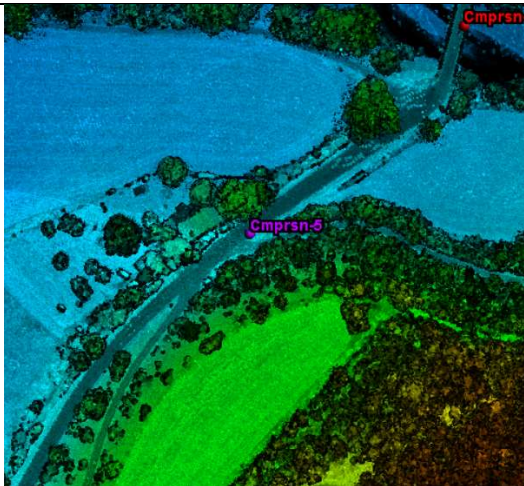


Figure 33 : Comparison point 5 from LIDAR



Figure 34 : Comparison point 5 from Photogrammetry

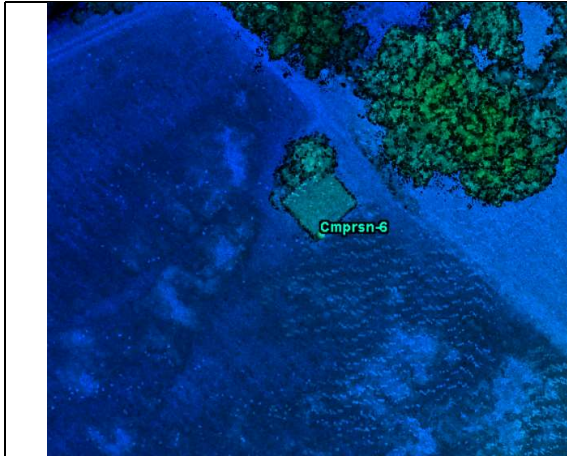


Figure 35 : Comparison point 6 from LIDAR



Figure 36 : Comparison point 6 from Photogrammetry

5. Discussion

This paper introduces a study utilizing multi-temporal UAV (Unmanned Aerial Vehicle) acquired images and the Structure from Motion (SfM) algorithm for mapping of river in order to see how morphology dynamics changed as well as quantifying bank erosion between 2023 and 2014 . In addition , suitability of UAV based data for monitoring river floodplain dynamics is addressed. UAVs offer a flexible, cost-effective, and precise means of data collection at centimeter resolution for specific target areas. Although processing numerous images can be computationally intensive, modern techniques enable fast, accurate, and straightforward analysis(Hemmelder et al., 2018). The SfM algorithm, known for its robustness, generates detailed and accurate outputs, provided there is substantial overlap (typically > 60%) among images, and the flight altitude aligns with the application, influencing spatial resolution(Yilmaz & Mahmud, 2018). In addition, LIDAR (Light Detection and Ranging) data serves as a reference dataset to validate the methods employed in this study. By comparing UAV-derived results with LIDAR data, researchers can evaluate the accuracy of UAV-based measurements in addition to that LIDAR data, offering high-resolution and precise topographic information, acts as a benchmark for validating UAV-based measurements(Cawood et al., 2017). This comparison enables researchers to quantify errors and uncertainties associated with UAV-based methods, assessing their reliability in monitoring and analyzing morphological changes within the study area.

After obtaining OrthoMosaics (5cm) and DEM(5cm), channel displacements ,erosion volume and retreatment is evaluated in this study. Between 2014 and 2015, channel displacement ranged up to 30 meters, while between 2022 and 2015, it reached up to 70 meters. Interestingly, there was minimal displacement between 2023 and 2022 despite observable changes in channel width. Elevation profiles derived from the DEMs have enabled the quantification of riverbank retreat due to erosion and sedimentation. Calculating bank erosion volumes is straightforward, typically involving subtracting DEMs from different years. However, the presence of trees and shrubs along the riverbank can obscure accurate elevation assessments, leading to uncertainties in volume estimates. To address this, an average height of the bank between vegetation was used as a reference height, providing a more accurate

assessment of eroded volume compared to subtracting DEMs with tree height. Bank erosion varied significantly between different time periods as well as offset of volumes resulted from average technique for height difference .Between 2015 and 2014, a river curve eroded over



an area of 170 by 45 meters with an estimated volume of $6040 \pm 492 \text{ m}^3$. Between 2022 and 2015, there were two eroded curves. The first extended 235 meters up to a maximum of 40 meters perpendicular to the channel, with an estimated volume of $15550 \pm 1174 \text{ m}^3$. The latter was easily calculated by subtracting the DEMs from 2022 to 2015 due to minimal vegetation cover, resulting in a computed volume of 5777 m^3 . The total area of both eroded parts is $21327 \pm 1174 \text{ m}^3$.

Figure 37 : Estimation of river boundary because of hampering by trees

Although discrepancies were observed in the bank line between 2023 and 2022, this resulted from

estimating the boundary, as direct drawing of bank lines was hindered by trees growing through the river. Bank line might be estimated as it is shown in *Figure 37* .Even if LIDAR point cloud were taken into consideration to distinguish bank line for 2023 , it is not possible to draw actual bank line. This problem is also encountered at the location of bridge. Even though estimated bank lines were drawn , there is not considerable differences observed (*Figure 38*). Thus , it can be deduced that there is not problematic situation occurred in this location.



Figure 38 : Bank lines at the location of bridge in every year , represented on Orthomosaic of 2023

This study area underwent annual image capture using Unmanned Aerial Vehicles (UAVs) from 2014 to 2023 , except for the years 2016 to 2021, during which no data was collected. Therefore , a challenge arises due to the disparity between the timescales of observation and actual change since bank erosion process take place in short surges during high discharge conditions. This limited

frequency of image acquisition makes it challenging to directly correlate mapped displacements and bank erosion with specific rainfall and discharge events. Researches assessing river morphology within broad time frame acquired more valuable result as they have more information about changes in every year. Wang et. al, (2020) carried out a research based on the long-term remote sensing image data between 1993 and 2016 in order to asses river morphology changes(Wang et al., 2020). Furthermore, Nath and

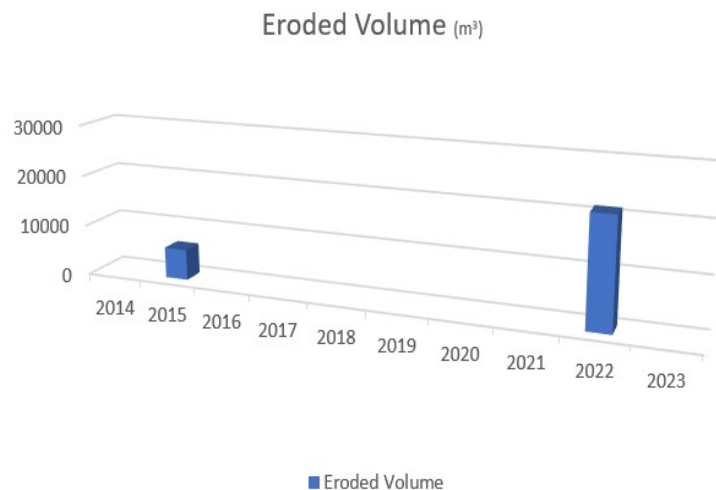


Figure 39: Eroded volume graph to show disconnected volume values

Gosh studied Barak River morphology changes from 1990 to 2020 (Nath & Ghosh, 2022).

Thus, it is concluded that river morphology changes should be monitored over a long period of time to acquire more valuable and accurate models serving as simplified representations of river systems, capturing the essential processes and characteristics influencing changes in river form and behavior. They create a controlled setting for studying river evolution (Coulthard & Van De Wiel, 2012). When it comes to outcomes of this study, there are missing values during the acquisition period. So, developing a comprehensive model is not ideal to forecast eroded volume or channel displacement. It is not applicable to form a regression model (Figure 39), since there is no information about which pattern erosion events follow from 2015 to 2022 and so on. If data had been available between these years, we could have found the relation and developed a model. Nonetheless, the methods outlined in this paper offer valuable insights for land managers and mapping agencies tasked with monitoring river dynamics and management. They could enhance monitoring efforts by implementing high-frequency UAV data collection campaigns or analyzing UAV images following significant discharge events.

The positional accuracy of our data varied between 7 to 9 cm horizontally and 3 to 12 cm vertically in comparison to Ground Control Points (GCPs) and their estimated positions in the model. The horizontal accuracy acquired from study conducted in La Batie in 2015 and 2014 developed in this paper since new co-alignment technique was applied thanks to data of additional surveys in 2022 and 2023. Thus, this level of accuracy proves both sufficient for our primary objective of erosion determination and its suitability for monitoring floodplain river. Vertical accuracy evaluation, conducted by contrasting LIDAR data with OrthoMosaic, exhibited a range of 3 to 9 cm. Over the course of our study, UAVs lacking RTK-GPS were utilized in 2014 and 2015, while newer models equipped with RTK-GPS were employed in 2022 and 2023. This upgrade significantly increased positional accuracy and mitigated the need for manual RTK-GPS measurements. The addition of more RTK-GPS points could have provided deeper insights into positional accuracy, thereby enhancing the overall quality of our assessment. Nevertheless, challenges persist, such as sun glint and mirroring effects in water channels, as well as obstacles like tumbled trees, which impede accurate channel depth interpretation. Uncertainties are multifaceted, with the magnitude often proving difficult to ascertain. Notably, camera quality plays a pivotal role, with consumer-grade cameras utilized in our UAVs. Upgrading to higher-quality cameras holds the potential for improved image quality, resulting in enhanced Digital Elevation Models (DEMs) and Mosaics due to superior calibration, diminished motion blur, and heightened contrast. Moreover, higher spatial resolution DEMs facilitate the detection of minuscule elevation changes over time. The field of UAV technology is rapidly evolving, with one of the most promising advancements being the development of fully autonomous drones. This innovation holds immense potential for river monitoring, allowing for more frequent and extensive data acquisition devoid of human intervention.

6. Conclusions

The utilization of Unmanned Aerial Vehicles (UAVs) in monitoring river dynamics and morphology has proven to be a highly effective and flexible approach. Through the application of multi-temporal UAV-acquired images and advanced algorithms like Structure from Motion (SfM), researchers have been able to analyze the changing morphology of rivers with remarkable precision and detail. This study underscores the value of UAV technology in providing centimeter-resolution (7 to 9 cm horizontally and 3 to 12 cm vertically) data for specific target areas, offering insights into channel displacements, erosion patterns, and bank retreat due to sedimentation. By comparing UAV-derived results with reference datasets like LIDAR, researchers can validate the accuracy of UAV-based measurements and quantify errors and uncertainties associated with the methodology. This study proved that there is consistency LIDAR and UAV based data in terms of accuracy. Despite challenges such as vegetation cover, the study demonstrates the reliability of UAV-derived data in monitoring and analyzing morphological changes within river systems. Furthermore, the study highlights the importance of long-term monitoring in understanding river dynamics accurately. While the limited frequency of image acquisition poses challenges in directly correlating mapped displacements with specific events, studies spanning broader timeframes provide valuable insights into morphological changes over time. Although there are opportunities for further enhancements, such as upgrading camera quality and utilizing fully autonomous drones, the current capabilities of UAV technology already offer significant benefits for river management. The ease of use, flexibility, and high spatial resolution of UAV images make them particularly valuable for monitoring small-scale changes and informing decision-making processes related to river administration and conservation.

In summary, the findings of this study affirm the suitability of UAV imagery for monitoring river dynamics and morphology, emphasizing its potential to revolutionize how we understand and manage river ecosystems in the future.

7. References

- Agisoft. (2023). *Metashape User Manual*. In (Version 2.0) https://www.agisoft.com/pdf/metashape-pro_2_0_en.pdf
- Akay, S. S., Ozcan, O., & Sen, O. L. (2019). Modeling morphodynamic processes in a meandering river with unmanned aerial vehicle-based measurements. *Journal of Applied Remote Sensing*, 13(4), 044523. <https://doi.org/10.1117/1.JRS.13.044523>
- Ashmore, P., & Church, M. (2001). The Impact of Climate Change on Rivers and River Processes in Canada. *Bulletin of the Geological Survey of Canada*, 1-48. <https://doi.org/10.4095/211891>
- Bertrand, M., Liébault, F., Brousse, G., Breilh, B., Laval, F., & Borgniet, L. (2018, 2018-10-24). *Hydromorphological restoration of the Upper Drac River IV* Convegno Italiano Riqualficazione Fluviale 2018, Bologne, Italy. <https://hal.science/hal-01982629>
- Cawood, A. J., Bond, C. E., Howell, J. A., Butler, R. W., & Totake, Y. (2017). LiDAR, UAV or compass-clinometer? Accuracy, coverage and the effects on structural models. *Journal of structural geology*, 98, 67-82.
- Colomina, I., & Molina, P. (2014). Unmanned aerial systems for photogrammetry and remote sensing: A review. *ISPRS Journal of Photogrammetry and Remote Sensing*, 92, 79-97. <https://doi.org/https://doi.org/10.1016/j.isprsjprs.2014.02.013>
- Coulthard, T. J., & Van De Wiel, M. J. (2012). Modelling river history and evolution. *Philosophical Transactions of the Royal Society A: Mathematical, Physical and Engineering Sciences*, 370(1966), 2123-2142. <https://doi.org/doi:10.1098/rsta.2011.0597>
- Cucchiaro, S., Cavalli, M., Vericat, D., Crema, S., Llena, M., Beinat, A., Marchi, L., & Cazorzi, F. (2018). Monitoring topographic changes through 4D-structure-from-motion photogrammetry: application to a debris-flow channel. *Environmental Earth Sciences*, 77(18), 632. <https://doi.org/10.1007/s12665-018-7817-4>
- Dimitriou, E., & Stavroulaki, E. (2018). Assessment of riverine morphology and habitat regime using unmanned aerial vehicles in a Mediterranean environment, Pure Appl. Geophys. <https://doi.org/https://doi.org/10.1007/s00024-018-1929-3>
- Duménieu, B., Abadie, N., & Perret, J. (2018). *Assessing the planimetric accuracy of Paris atlases from the late 18th and 19th centuries* Proceedings of the 33rd Annual ACM Symposium on Applied Computing, Pau, France. <https://doi.org/10.1145/3167132.3167228>
- Feurer, D., & Vinatier, F. (2018). Joining multi-epoch archival aerial images in a single SfM block allows 3-D change detection with almost exclusively image information. *ISPRS Journal of Photogrammetry and Remote Sensing*, 146, 495-506. <https://doi.org/https://doi.org/10.1016/j.isprsjprs.2018.10.016>
- Hemmelder, S., Marra, W., Markies, H., & De Jong, S. M. (2018). Monitoring river morphology & bank erosion using UAV imagery – A case study of the river Buëch, Hautes-Alpes, France. *International Journal of Applied Earth Observation and Geoinformation*, 73, 428-437. <https://doi.org/https://doi.org/10.1016/j.jag.2018.07.016>
- Hooke, J. M. (1979). An analysis of the processes of river bank erosion. *Journal of hydrology*, 42(1-2), 39-62. Institut National De L'Information Geographique Et Forestiere. IGN. <https://geoservices.ign.fr/lidarhd>
- Julzarika, A. (2019). FREE GLOBAL DEM: CONVERTING DSM TO DTM AND ITS APPLICATIONS. *ISPRS - International Archives of the Photogrammetry, Remote Sensing and Spatial Information Sciences*, XLII-4/W16, 319-325. <https://doi.org/10.5194/isprs-archives-XLII-4-W16-319-2019>
- Kabdaşlı, S. (2010). Karasu Sahili Erozyon Probleminin İncelenmesi-Ön Değerlendirme Raporu. İTÜ İnşaat Fakültesi, Su ve Deniz Bilimleri ve Teknolojisi Uygulama ve Araştırma Merkezi.
- Lewin, J., Brewer, P. A., & Wohl, E. (2018). Fluvial Geomorphology. In *Reference Module in Earth Systems and Environmental Sciences*. Elsevier. <https://doi.org/https://doi.org/10.1016/B978-0-12-409548-9.11108-X>

- Li, W., Colombera, L., Yue, D., & Mountney, N. P. (2023). Controls on the morphology of braided rivers and braid bars: An empirical characterization of numerical models. *Sedimentology*, 70(1), 259-279. <https://doi.org/https://doi.org/10.1111/sed.13040>
- Li, Z., Zhu, C., & Gold, C. (2004). *Digital terrain modeling: principles and methodology*. CRC press.
- Liébault, F., Lallias-Tacon, S., Cassel, M., & Talaska, N. (2013). LONG PROFILE RESPONSES OF ALPINE BRAIDED RIVERS IN SE FRANCE. *River Research and Applications*, 29(10), 1253-1266. <https://doi.org/https://doi.org/10.1002/rra.2615>
- Makaske, B. (2001). Anastomosing rivers: a review of their classification, origin and sedimentary products. *Earth-Science Reviews*, 53(3), 149-196. [https://doi.org/https://doi.org/10.1016/S0012-8252\(00\)00038-6](https://doi.org/https://doi.org/10.1016/S0012-8252(00)00038-6)
- McGrane, S. J. (2016). Impacts of urbanisation on hydrological and water quality dynamics, and urban water management: a review. *Hydrological Sciences Journal*, 61(13), 2295-2311. <https://doi.org/10.1080/02626667.2015.1128084>
- Meinen, B. U., & Robinson, D. T. (2020). Streambank topography: an accuracy assessment of UAV-based and traditional 3D reconstructions. *International Journal of Remote Sensing*, 41(1), 1-18. <https://doi.org/10.1080/01431161.2019.1597294>
- Monegaglia, F., & Tubino, M. (2019). The hydraulic geometry of evolving meandering rivers. *Journal of Geophysical Research: Earth Surface*, 124(11), 2723-2748.
- Nath, A., & Ghosh, S. (2022). Assessment of river morphology based on changes in land use and land cover and the spatial and temporal variation of meandering parameters of the barak river. *Water Practice and Technology*, 17(11), 2351-2370. <https://doi.org/10.2166/wpt.2022.114>
- Nota, E. W., Nijland, W., & de Haas, T. (2022). Improving UAV-SfM time-series accuracy by co-alignment and contributions of ground control or RTK positioning. *International Journal of Applied Earth Observation and Geoinformation*, 109, 102772. <https://doi.org/https://doi.org/10.1016/j.jag.2022.102772>
- Pędzich, P. (2005). Conformal projection with minimal distortions. XXII International Cartographic Conference Proceedings", La Coruna,
- Pineux, N., Lisein, J., Swerts, G., Bielders, C. L., Lejeune, P., Colinet, G., & Degré, A. (2017). Can DEM time series produced by UAV be used to quantify diffuse erosion in an agricultural watershed? *Geomorphology*, 280, 122-136. <https://doi.org/https://doi.org/10.1016/j.geomorph.2016.12.003>
- Ramalingam, S., Lodha, S. K., & Sturm, P. F. (2006). A generic structure-from-motion framework. *Comput. Vis. Image Underst.*, 103, 218-228.
- Saponaro, M., Capolupo, A., Caporusso, G., & Tarantino, E. (2021). INFLUENCE OF CO-ALIGNMENT PROCEDURES ON THE CO-REGISTRATION ACCURACY OF MULTI-EPOCH SFM POINTS CLOUDS. *Int. Arch. Photogramm. Remote Sens. Spatial Inf. Sci.*, XLIII-B2-2021, 231-238. <https://doi.org/10.5194/isprs-archives-XLIII-B2-2021-231-2021>
- Sonam, Jain, V., Fryirs, K., & Brierley, G. (2022). Geomorphic characterization of a seasonal river network in semi-arid western India using the River Styles Framework. *Journal of Asian Earth Sciences*: X, 7, 100077. <https://doi.org/https://doi.org/10.1016/j.jaesx.2021.100077>
- Sui-ji, W., & Jin-ren, N. (2002). Straight river: its formation and speciality. *Journal of Geographical Sciences*, 12, 72-80.
- Tang, Q., Schilling, O. S., Kurtz, W., Brunner, P., Vereecken, H., & Hendricks Franssen, H.-J. (2018). Simulating Flood-Induced Riverbed Transience Using Unmanned Aerial Vehicles, Physically Based Hydrological Modeling, and the Ensemble Kalman Filter. *Water Resources Research*, 54(11), 9342-9363. <https://doi.org/https://doi.org/10.1029/2018WR023067>
- Vannamettee, E. (2014). *Hydrograph prediction in ungauged basins: Development of a closure relation for Hortonian runoff*. Utrecht University.
- Vita-Finzi, C. (2012). River history and tectonics. *Philosophical Transactions of the Royal Society A: Mathematical, Physical and Engineering Sciences*, 370(1966), 2173-2192. <https://doi.org/doi:10.1098/rsta.2011.0605>

- Wang, P., Fu, K., Huang, J., Duan, X., & Yang, Z. (2020). Morphological changes in the lower Lancang River due to extensive human activities. *PeerJ*, 8, e9471. <https://doi.org/10.7717/peerj.9471>
- Yilmaz, H. M., & Mahmud, A. A. (2018). İnsansız Hava Aracı İle Dik Konumda Çekilen Resimlerle Üç Boyutlu Model Oluşturma: Aksaray Üniversitesi Kampüs Camii [Generating to Three Dimensional Models from Taken Photos in Vertical Position with Unmanned Aerial Vehicles: Aksaray University Campus Mosque]. *Aksaray University Journal of Science and Engineering*, 2(2), 144-160. <https://doi.org/10.29002/asujse.387797>
- Zarrabi, N., Moghim, M. N., & Eftekhar, M. R. (2021). Effect of hydraulic parameters on abrasion erosion of fiber reinforced concrete in hydraulic structures. *Construction and Building Materials*, 267, 120966. <https://doi.org/https://doi.org/10.1016/j.conbuildmat.2020.120966>
- Zhang, J., Boutin, M., & Aliaga, D. G. (2006, 8-11 Oct. 2006). Robust Bundle Adjustment for Structure from Motion. 2006 International Conference on Image Processing,